Boillot, G., Winterer, E. L., et al., 1988
Proceedings of the Ocean Drilling Program, Scientific Results, Vol. 103

6. MICROFACIES OF UPPER JURASSIC LIMESTONES, ODP SITE 639[1]

Michel Moullade, Laboratoire de Micropaléontologie et Géologie Marines, Université de Nice, Nice, France
Jean-Paul Loreau, Centre des Sciences de la Terre, Université de Bourgogne, Dijon, France
Jürgen Thurow, Institut und Museum für Geologie und Paläontologie, Universität Tübingen, Tübingen, Federal Republic of Germany
Pierre Cros, Laboratoire de Stratigraphie de l'Université Pierre et Marie Curie, Paris, France
and
Michel Cousin, Laboratoire de Géodynamique Sous-Marine, Villefranche-sur-Mer, France

ABSTRACT

A detailed analysis of the texture, matrix, and elements of the microfacies from the carbonate sequence recovered in ODP Hole 639D resulted in a typological classification of 10 major microfacies types and their variants. The variations in distribution and succession of type microfacies allowed us to divide the carbonate sequence into 12 facies-defined subunits. Based on the analyzed characteristics and their relations, we also propose a paleoenvironmental interpretation involving a mixed carbonate/terrigenous ramp model instead of the previous, classical zoned carbonate platform.

INTRODUCTION

During Ocean Drilling Program (ODP) Leg 103, several attempts were made to penetrate and core the Jurassic carbonate layer inferred to occur at several tilted blocks on the Galicia margin from seismic profiles and previously recovered dredge samples. Hole 639D (42°08.6'N, 12°15.3'W; 4748 m water depth; Fig. 1) was the most successful attempt at this endeavor; 13 cores were recovered from the hole, but typically, recovery was poor. The uppermost wash core (Core 103-639D-1W) consists of Neogene-Quaternary clay, whereas Core 103-639D-2R through part of Core 103-639D-4R contain dolomite. The remaining nine cores (Cores 103-639D-5R through 103-639D-13R) consist almost exclusively of limestone, interbedded with sandstone in Cores 103-639D-7R and 103-639D-8R. The foraminiferal assemblages found in the limestone section indicate a latest Jurassic age. A more precise late Tithonian age is suggested from rare, usually poorly preserved calpionellids (see "Site 639" chapter; Shipboard Scientific Party, 1987).

In this study, we used thin sections to analyze and define the various microfacies observed in the limestone and associated sandstone section. The dolomite interval is only briefly described here, as it is the subject of another paper in this volume (Loreau and Cros). Our study combined sedimentologic and paleontologic approaches in an attempt to reconstruct the environment of deposition of the various carbonate microfacies deposited during the late Tithonian on this part of the Galicia margin.

DESCRIPTION AND DISTRIBUTION OF MICROFACIES BASED ON THIN-SECTION ANALYSIS

Classification Criteria

Texture

We used Dunham's (1962) classification, emended by Embrie and Klovan (1971), to describe the texture of the recovered carbonate rocks. The term "micropackstone" was added (Loreau, 1982) to describe the grain-supported texture of a fine-grained sediment (or the fine fraction of a heterometric sediment) consisting of grains smaller than 100 μm and closely packed in micrite.

Textures observed in the cores include mudstones, wackestones, floatstones, micropackstones, heterometric packstones (95% of which have a micropackstone matrix), and relatively rare grainstones. Textural variations sometimes occurred within the same thin sections.

Elements

Areal percentages of the grains, biogenic debris, and organisms in each thin section were estimated by visual examination of their relative proportions (Fig. 2). Organisms, elements resulting from biogenic activity, and detrital grains are the three main categories distinguished on the basis of their nature and/or size.

Organisms

Six organism categories were distinguished:

1. Tiny organisms usually found in abundance in open environments (e.g., outer platform), such as calpionellids, thin calcitic pelecypod shells, and calcitized spicules of siliceous sponges.
2. Benthic foraminifers, including large agglutinated and/or microgranular foraminifers (*Anchispirocyclina lusitanica*, *Pseudocyclammina lituus*, and *Pseudocyclammina* sp.), small agglutinates (*Textulariidae*, *Verneuilinidae*, *Ataxophragmiidae*, etc.), small imperforates (*Nautiloculina oolithica* and *Miliolidae*), and small calcareous benthic foraminifers (*Trocholina* gr. *alpina-elongata*, *Epistomina* spp., and *Lenticulina* spp.).
3. Echinoderms, including Ophiurids, *Spatangus*-type, and Echinid-type radiols (cf. Lucas et al., 1976), and unspecified echinoderm debris.
4. Mollusks (pelecypods and gastropods) and brachiopods.
5. Algae (Pls. 13 through 15), consisting primarily of green algae such as *Udoteaceae* (*Arabicodium* or *Boueina*) and *Dasycladaceae* (bioclasts of *Clypeina*, *Pseudoclypeina*, *Salpingoporella*, *Cylindroporella*, and *Griphoporella*). Secondary varieties are some red algae (*Melobesiae* and *Gymnocodiaceae*) and structures made by blue-green algae, such as stromatolitic encrustations and *Bacinella/Lithocodium* features, which are interpreted

[1] Boillot, G., Winterer, E. L., et al., 1988. *Proc. ODP, Sci. Results*, 103: College Station, TX (Ocean Drilling Program).

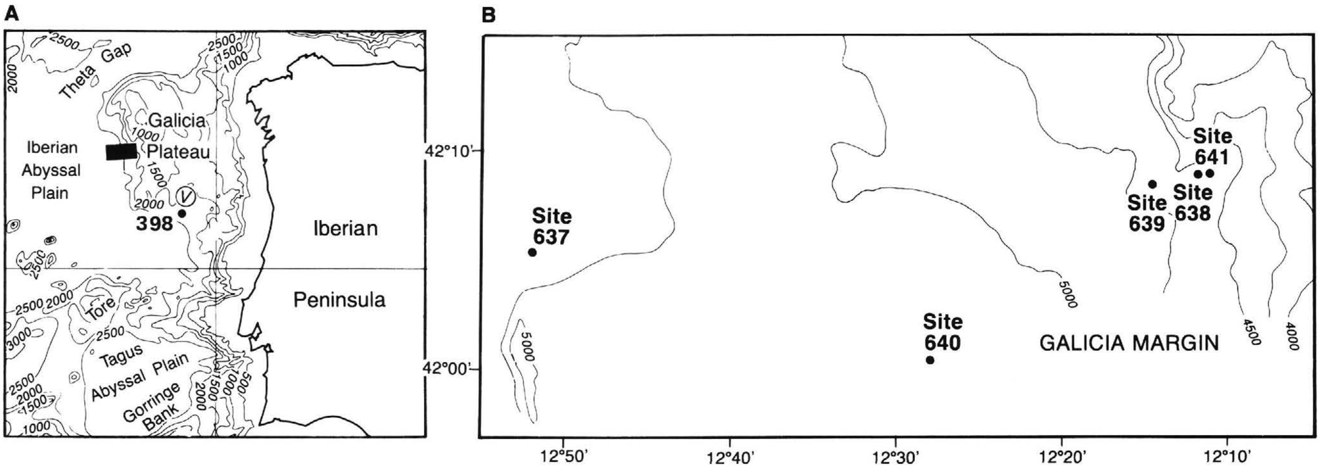

Figure 1. Location of ODP Leg 103 drill sites along the Galicia margin. Bathymetry in meters. Solid rectangle in Figure 1A shows area covered by Figure 1B.

as Cyanophycean (or Cyanobacterian) constructions unless they are attributed to the Stromatoporidean group.

6. Typical reef-building organisms, including corals, calcareous sponges (Pharetrones in Pl. 7, Fig. 1; Chaetetids in Pl. 6 and Pl.. 7, Fig. 3), and bryozoans.

Ostracodes were also identified in thin section but, because of their rarity, we did not distinguish them as a separate group.

Elements Resulting from Biogenic Activity

These elements include the following:

1. Encrustations of plurimillimetric bioclastic grains or entire shells and skeletons. These micritic features are secreted by either porcelaneous (*Nubecularia*) or hyaline foraminifers (Pl. 8, Fig. 2), serpulids, and bryozoans.

2. Coated grains (oncoids), either rounded or irregular, that are generally 1-3 mm in size (maximum = 5 mm). These grains have a homogeneous or laminated micritic cortex displaying foraminiferal(?) chambers and other probable microscopic organisms.

3. Composite grains (grapestones), commonly composed of several oncoids or other grains such as pellets and foraminifers (Pl. 1, Figs. 1 through 4).

Detrital Grains

Quartz and feldspar are the siliceous clastics comprising the detrital grains category.

Matrix

Two kinds of matrix are present in the Hole 639D samples:

1. Matrix with a dominantly micritic texture, either strictly micritic or "clotted" (i.e., including obscure microelements and microspar in the micritic background; Pl. 4, Fig. 2). This kind of matrix usually includes dispersed and very fine-grained bioclastic debris.

2. Matrix with a micropackstone texture (Pl. 3), composed of micritic pellets 50–100 μm in size, small agglutinated or porcelaneous or (rarely) calcareous perforate few-chambered foraminifers, and small (some tens of microns) bioclastic debris. The microdebris are recrystallized, either hardly identifiable or of the same nature as the large debris (pelecypods and algae). Sometimes the microdebris are so dense that this matrix is equivalent to a bioclastic micropackstone. Small micritic pellets are dominant locally. The small micritic pellets have three appearances under the microscope: (a) gray tint + rounded morphology + blurred boundaries (Pl. 12, Fig. 3), (b) dark tint + rounded morphology + clear boundaries (Pl. 4, Fig. 1), or (c) variable tint + irregular polygonal morphology (Pl. 4, Fig. 3) + usually clear boundaries. These three micropellet types are commonly mixed within a thin section (Pl. 3 and Pl. 4, Figs. 1 and 3). Such features imply an *in-situ* diagenetic evolution (Pl. 4, Fig. 3). However, these pellets are not to be confused with the small micritized debris ("pelletoids") associated with larger micritized bioclasts showing all medium sizes and morphologies (Pl. 4, Figs. 1 and 4).

Microfacies Types

Combining the information on texture, matrix, and elements of the studied thin sections permitted us to define 10 main microfacies categories for the carbonate rocks of Hole 639D. Some of these categories are further subdivided into subtypes or variants on the basis of minor variations in their characteristics.

1. Heterometric Packstone with Oncoids and Large Foraminifers (Fig. 3)

Within a micropackstone texture matrix, the dominant, usually supported grains are oncoids (up to 20%; rounded and irregular oncoids vary in abundance) and large foraminifers (up to 5%) (*Anchispirocyclina* and *Pseudocyclammina*). Algae and pelecypod debris and *Trocholina* are accessory allochems.

Based on their size (few are ≥5 mm), the oncoids are similar to ooids and, as such, should be named "micro-oncoids." The nuclei are large foraminifers, pelecypod fragments, or, rarely, small (1-mm) pieces of a gastropod, coral, serpulid, or a grapestone; the cortex consists of undifferentiated or laminated micrite. Laminations are distinguished by different optic densities of micrite or by the presence of associated encrusting organisms, mainly *Nubecularia* s.l. The presence of algal filaments is questionable. The shape of the nucleus determines the external morphology of the oncoid, because the cortex has an almost constant thickness. The largest (5-mm) oncoids are commonly irregular, the extreme case being those formed around centimeter-sized elongated debris of pelecypods. In addition, the surface of the oncoid can be irregular because of the presence of well-preserved encrusting foraminifers. The regular rounded morphology depends not only on the globular shape of the nucleus (especially foraminifers) but also is a result of the compensating variations of thickness of the cortex; small nuclei of irregular shape tend to be ovoid or subspherical.

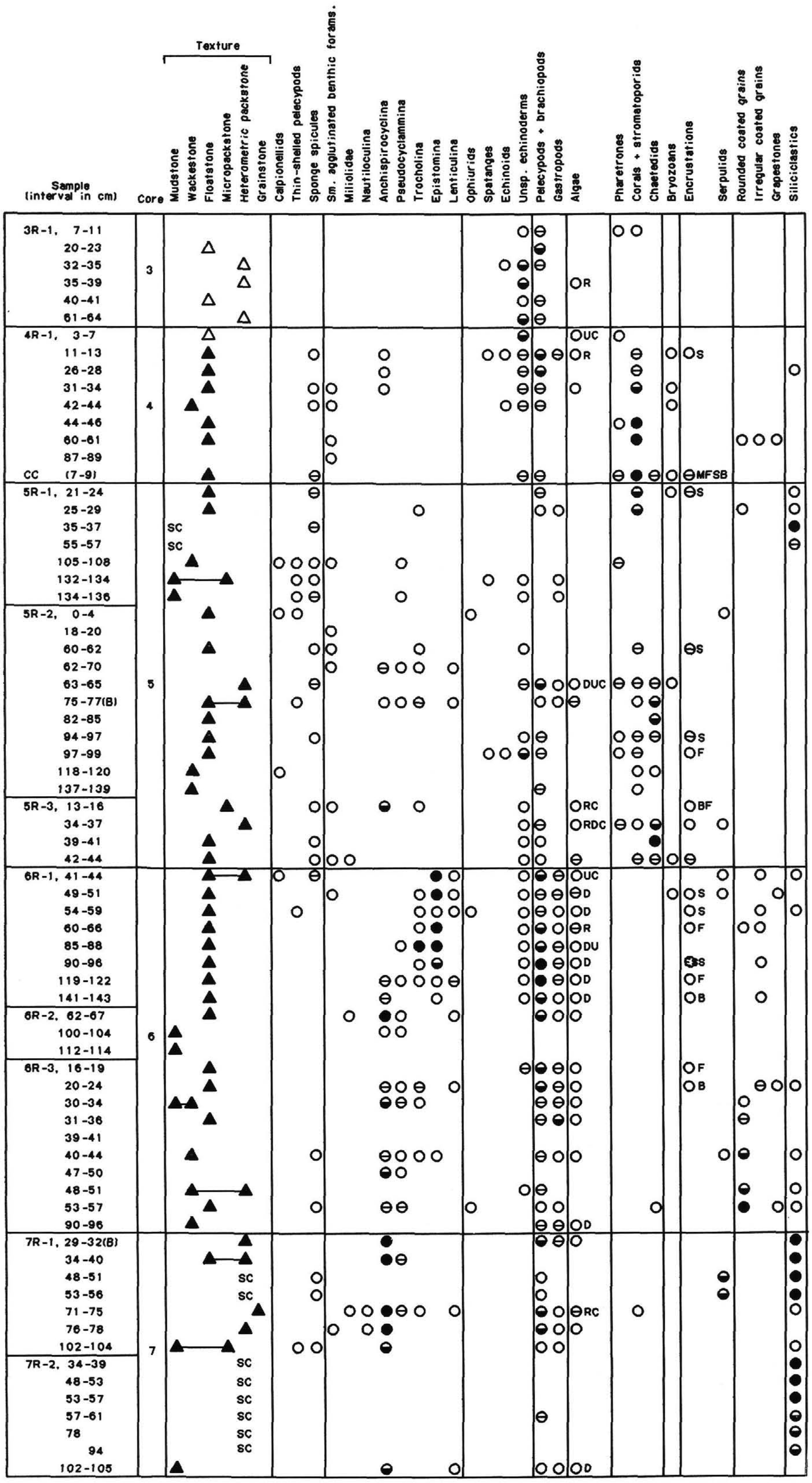

Figure 2. Distribution of textures and elements observed in thin sections, Hole 639D. Texture: solid triangle (open when supposed). SC = siliciclastics. Elements: open circle = <1%, divided circle = 1%–5%, half-solid circle = 5%–20%, solid circle = >20%. Algae: C = Chlorophyceae, D = Dasycladaceae, U = Udotheaceae, R = Rhodophyceae. Encrustation: M = micrite, F = foraminifer, S = serpulid, B = bryozoan.

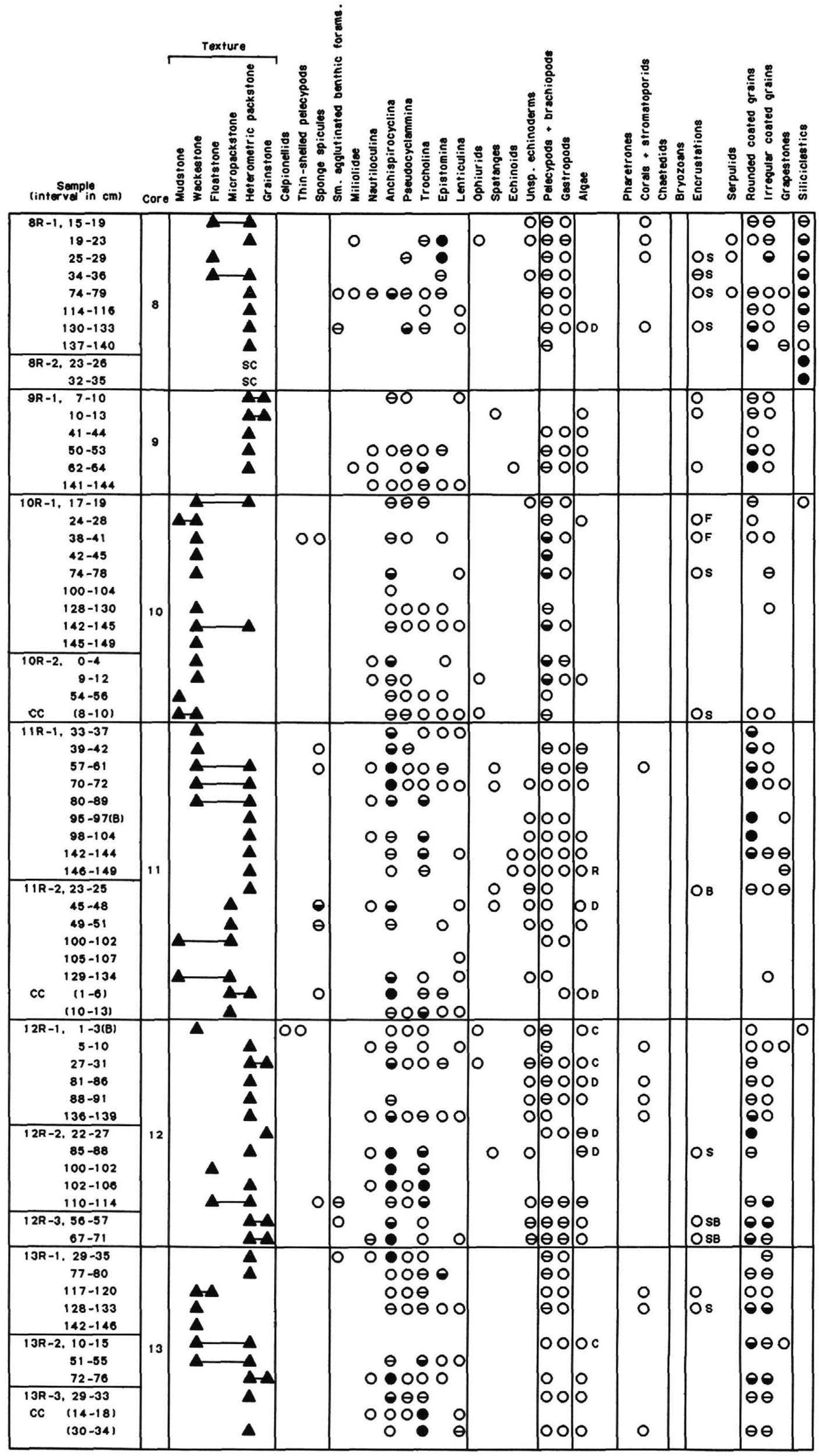

Figure 2 (continued).

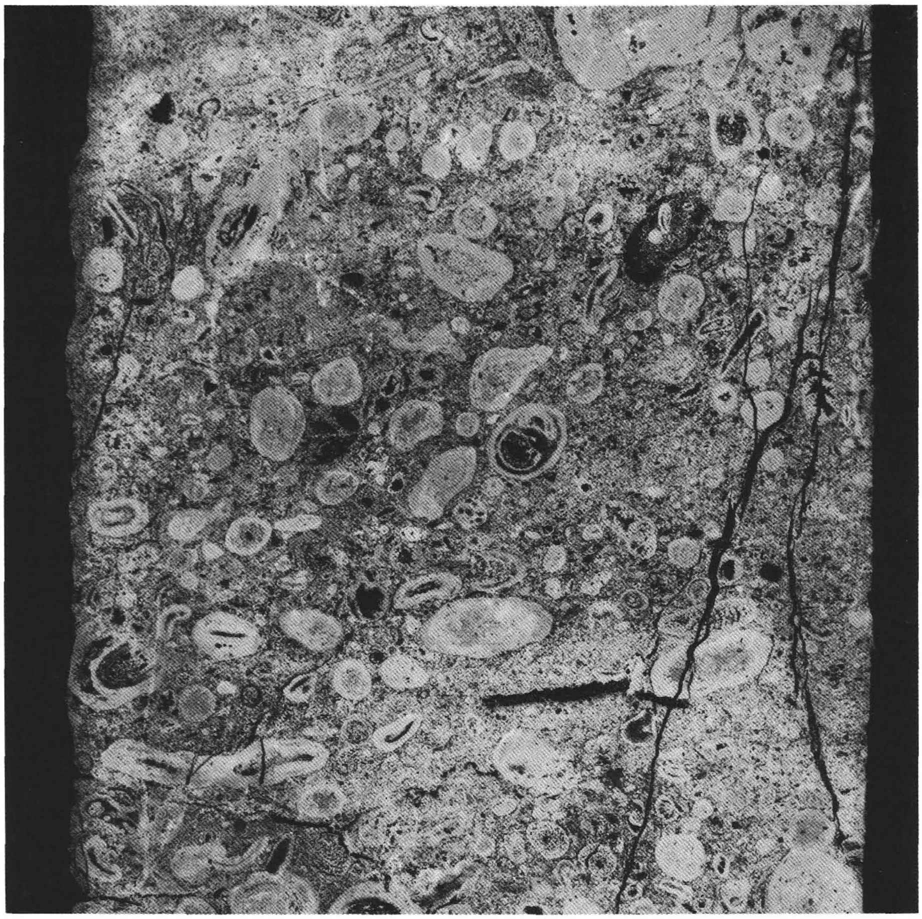

Figure 3. Heterometric packstone with oncoids and large foraminifers. Oncoids are irregular with various nuclei, including serpulids, pelecypod shells, and composite grains. The micritic cortex shows chambers of *Nubecularia*. The matrix is a micropackstone. Sample 103-639D-12R-3, 67–71 cm (negative print from thin section, 6.5X).

The various shapes, sizes, and mixtures of oncoids in this microfacies type suggest differing degrees of hydrodynamic energy and a significant influence from bioturbation (Fig. 4; see following discussion).

2. Heterometric Packstone with Oncoids (Fig. 5)

Like the preceding heterometric packstone with oncoids and large foraminifers, this microfacies type is also bimodal; oncoids are the dominant allochems, floating within a micropackstone texture matrix. Most of the foraminifers are coated. Accessory grains include echinoderm, pelecypod, gastropod, algae, and coral debris. This microfacies type has two subdivisions.

The first subdivision is a heterometric packstone with oncoids and associated grapestones (Pl. 1, Fig. 1). These oncoids are usually well sorted and grain supported within a micropackstone texture matrix. Grapestones and composite grains show all of the intermediate stages in terms of structure and alteration. They tend either to become oncoids when the aggregate has been subjected to coating or to develop as cryptocrystalline grains as a result of micritization (Pl. 1, Fig. 2). Some include cavities with circular cross sections, filled by microspar (Pl. 1, Fig. 4).

The second subdivision of this category is defined by the presence of fine-grained quartz within the matrix, trapped within oncoids, and incorporated with the walls of agglutinated foraminifers (Pl. 1, Fig. 3, and Pl. 2, Fig. 1). The features of this subdivision suggest a unique environment for the genesis of oncoids, the life cycle of foraminifers, and the deposition of silt, as we subsequently discuss.

3. Wackestone-Floatstone with Oncoids, Large Foraminifers and Mollusk Bioclasts (Fig. 6)

The third microfacies type differs from the heterometric packstone in texture (increased micrite content), composition of the matrix (micritic and without a micropackstone texture), and the significant presence of bioclasts (gastropods and calcitic pelecypods). Accessory components are algae, a few *Trocholina*, and rare quartz grains. This microfacies type is subdivided into a microfacies characterized by a distinct decrease in the abundance of oncoids and a significant content of gastropods (Fig. 7) and a second microfacies that has relatively more micrite and fewer oncoids and mollusk bioclasts (Fig. 8).

Rare depositional and diagenetic decreases in the significance of the matrix cause this microfacies type to resemble a heterometric grainstone.

4. Wackestone-Floatstone with Pelecypods and Large Foraminifers (Fig. 9)

This microfacies resembles the preceding wackestone-floatstone except that it does not contain oncoids. The strictly micritic, or slightly clotted, matrix of this microfacies type contains abundant bioclastic microdebris. Dominant allochems in-

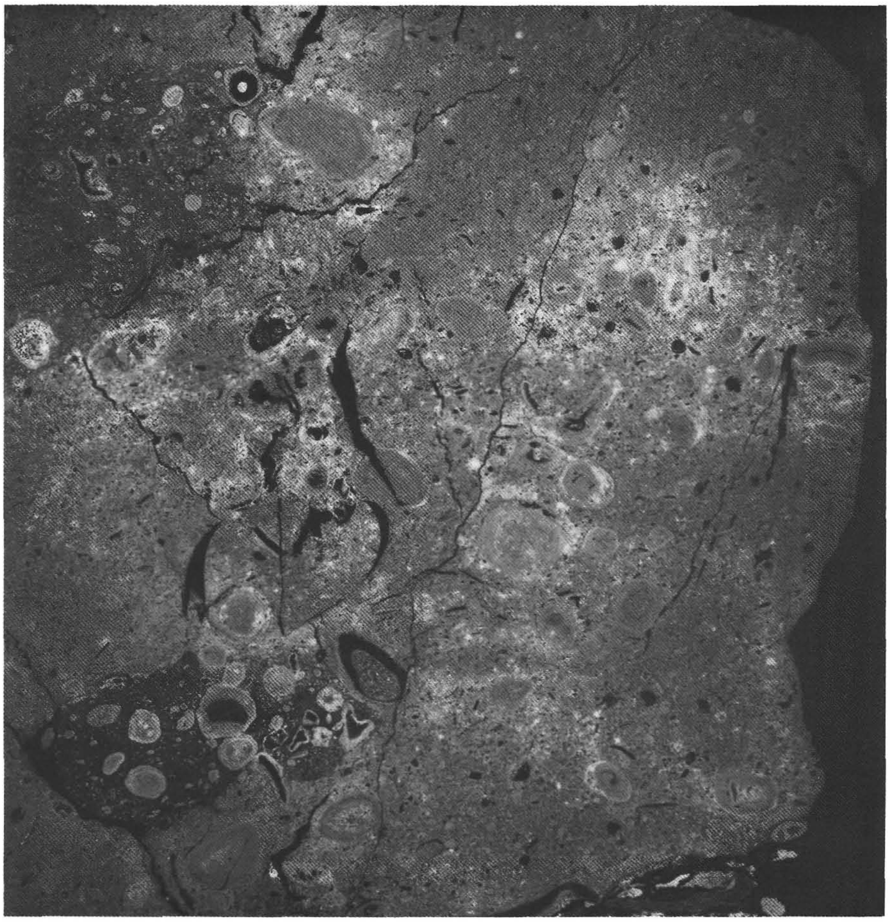

Figure 4. Aspects of microfacies showing different types of textures and various shapes, sizes, and mixtures of oncoids suggesting a significant influence of bioturbation. Sample 103-639D-13R-1, 77–80 cm (negative print from thin section, 6.5X).

clude the debris of calcitic fibrous pelecypods (some are centimeter sized, broken, bored, and partially micritized) and large benthic foraminifers. Gastropod fragments are accessory components.

Three variants of this microfacies are observed: (1) with pelecypod accessory elements (Fig. 7), (2) with allochems comprising less than 10% of the thin section (mudstone), and (3) with a micropackstone texture matrix occurring locally within the same thin section.

5. Micropackstone with Large Foraminifers and Sponge Spicules (Pl. 3, Fig. 1)

The matrix of the fifth microfacies type has a dominantly micropackstone texture and contains large foraminifers and calcitized spicules of siliceous sponges but no oncoids. Rarely present are the debris of echinoderms (especially *Spatangus*-type radiols), pelecypods, and algae. Variations within the microfacies depend on texture; locally present micritic matrix distinguishes a "mudstone-wackestone with large foraminifers and sponge spicules."

6. Wackestone-Floatstone with Algae and Mollusks (Fig. 8)

The micritic matrix of this wackestone-floatstone (with microbioclasts and various smaller benthic foraminifers) contains bioclastic debris, typically of millimeter—with some occurrences up to centimeter—size. This debris consist of pelecypods, various mollusks, and red and green algae (*Dasycladaceae* and *Udoteaceae*). Echinoderms and large foraminifers are accessory allochems. This microfacies is similar to the wackestone-floatstone with pelecypods and large foraminifers microfacies (type 4), but the foraminifers are less numerous, whereas the algae are much more abundant.

Some of the thin sections classified under this category are characterized by >1% large foraminifers, but the absence of oncoids still differentiates this composition from the wackestone-floatstone with oncoids, large foraminifers, and mollusk bioclasts microfacies (type 3).

7. Heterometric Grainstone with Pelecypods and Large Foraminifers (Fig. 10)

This microfacies type is characterized by a heterometric grainstone texture with imbricated bedding. It is composed of centimeter-sized, usually micritized, and rounded debris of pelecypods and of well-preserved or only slightly eroded large foraminifers. Small, rounded, highly micritized grains are positioned interstitially. Accessory components include algae and coral debris and a few quartz grains.

8. Floatstone with Small Corals and Calcareous Sponge Debris (Pl. 5, Fig. 1, and Pl. 6, Figs. 1 and 2)

Thin sections of this floatstone microfacies type show a micritic matrix containing abundant microbioclasts, a few small agglutinated benthic foraminifers, calcitized spicules of siliceous sponges (Pl. 9, Fig. 5), and rare calpionellids. Most of the bioclastic allochems and organisms previously mentioned are present within the matrix, including (1) echinoderms, progressively in-

Figure 5. Heterometric packstone with oncoids dominating the allochems dispersed in a micropackstone matrix. Foraminifers are exceptionally devoid of coatings. Accessory grains are echinoderm, pelecypod, gastropod, algae, and coral debris. Sample 103-639D-12R-3, 67–71 cm (negative print from thin section, 6.5X).

creasing in abundance (up to 20%) toward the top of the limestone sequence; (2) mollusks (pelecypods and rare gastropods) and brachiopods (Pl. 9, Fig. 1); and (3) algae as an accessory of about 1%. Oncoids and grapestones are absent. Other debris are 1 mm to 3–4 cm in size and include corals, calcareous sponges, such as Chaetetids (J. C. Fischer, pers. comm., 1986; Fischer, 1970; Cuif et al., 1973) and Pharetrones (Pl. 5, Fig. 3, Pl. 6, Fig. 2, and Pl. 7, Fig. 1). Accessory components include circular sections of tubicole annelids (Pl. 8, Fig. 4) and lithistid sponge debris that have experienced early diagenesis into micrite and sparite ("tuberoids"; cf. Fritz, 1958; Gaillard, 1983) (Pl. 7, Fig. 3). Large foraminifers are very rare.

Some of the coral and Chaetetid debris are bored, encrusted, and generally reworked. The reworking seems to have occurred *in situ*, that is, to be biological. Encrustations, some of which are polyphased (Pl. 8, Fig. 1), are built by laminated or undifferentiated micrites, stromatoporids(?) (Pl. 8, Fig. 2), foraminifers, serpulids, bryozoans, *Rhodophyceae* (Pl. 8, Fig. 3), and sponges.

Evidence of early lithification within the micritic matrix is also observed (see Loreau and Cros, this volume). Significant fracturing of the rock, leading to tectonic brecciation, may obscure the initial texture (Pl. 6, Fig. 2). A variant of this microfacies type has a micropackstone matrix developed from an increase in microbioclasts, which results in local occurrences of a heterogeneous packstone consisting of the same elements.

9. Siliciclastics

Sandstones, silts, and colored clays are interbedded in the limestone sequence of Hole 639D (Shipboard Scientific Party, 1987). The heterometric sandstones (Pl. 2, Fig. 2) consist of angular quartz grains (some plurimillimetric) and accessory feldspars, lithic fragments, and rare calcitic pelecypod debris in a yellowish red micritic matrix rich in quartz silt and 10–30-μm-size dolomite crystals. Some of the sandstones have a dolomitic cement. The quartz silts have a fine argillaceous-carbonate matrix and contain other calcareous, bedded allochems, such as bioclastic debris (usually pelecypods), large agglutinated foraminifers, and elongated micritic intraclasts.

10. Dolomites

The ghosts of bioclasts in the crystalline dolomite microfacies suggest initial textures that might have been either a floatstone-packstone or possibly a grainstone. Identifiable bioclasts are mainly debris of echinoderms (supposedly more resistant to recrystallization), pelecypods, gastropods, algae, calcareous sponges (pharetrones), and, in exceptionally rare cases, foraminifers (fragments of *Anchispirocyclina*; Pl. 10, Fig. 1).

Association and Distribution of Microfacies

The stratigraphic succession based on the dominant microfacies in Hole 639D is roughly divided into an oncoid-bearing se-

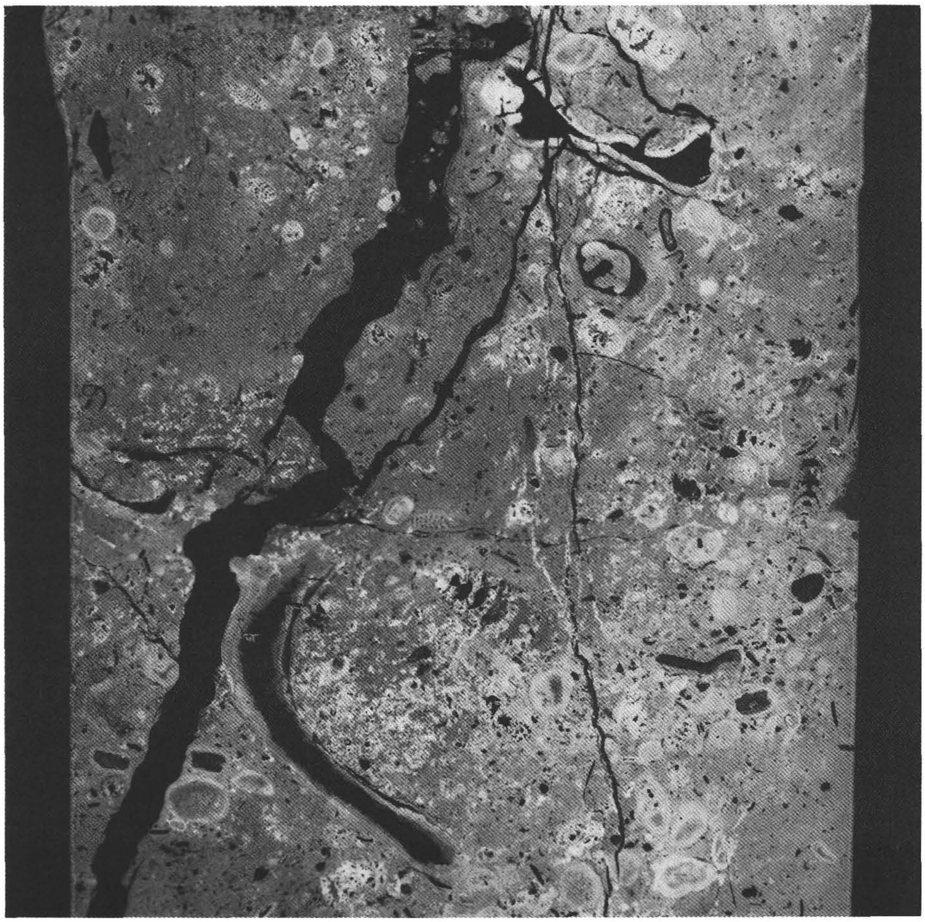

Figure 6. Wackestone-floatstone with oncoids, large foraminifers, and mollusk bioclasts. The microfacies has a dominantly micritic matrix and a significant amount of bioclasts (pelecypods and gastropods; minor constituents include algae, *Trocholina*, and rare quartz grains). Sample 103-639D-6R-3, 20–24 cm (negative print from thin section, 6.5X).

quence at the base of the section and a sequence with small sessile organisms (corals and sponges) at the top, separated by an intermediate, mostly detrital, interval (see also "Site 639" chapter; Shipboard Scientific Party, 1987). However, transitions and facies recurrences are common; second-order boundaries within the main units are recognized by the appearance or disappearance of one or more biogenic elements. Some of these boundaries are artificially exaggerated, as they coincide with gaps resulting from insufficient core recovery. Twelve subunits (*a–l*), characterized by one or a few dominant microfacies types, were thus defined (see details in Fig. 11). Subunits *a* through *e*, in which microfacies types 1, 2, 4, and 5 are dominant, belong to the "lower oncoidal limestones"; subunits *f* through *j*, characterized mainly by microfacies types 2, 3, 5 through 7, and 9, are grouped together as "middle sandstones and clayey limestones"; subunit *k*, in which microfacies type 8 is dominant, corresponds to the "upper clayey limestones"; and subunit *l* represents the overlying dolomite section.

Distribution of Microfaunal Assemblages (Fig. 2)

Calpionellids are very rare, and generally badly preserved, throughout the section drilled at Hole 639D. However, calpionellids were found to be slightly more abundant in subunits *i* and *k*. Anchispirocyclines are abundant in subunits *a* through *e*, the upper part of *h*, *i*, and the lower part of *j*. They are rare in the upper part of the section (the upper part of subunit *j* and subunit *k*). Trocholines, Pseudocyclammines, and Nautiloculines also show a clear decrease in abundance toward the top of the section. In addition, two significant peaks appear in the distribution of Epistominids in subunits *g* and *j*.

DISCUSSION: ELEMENTS FOR A SEDIMENTARY MODEL

Classical (Zoned) Carbonate Platform?

The nature and distribution of the various microfacies observed in Hole 639D do not support interpretation of the sequence as a classical carbonate platform, because they do not include an outer sandy facies (e.g., oolites, bioclastic grainstones, or coralline sands) or a confined peritidal facies, nor do they show evidence of a possible reefal barrier. Instead, as a preliminary working hypothesis, we suggest that the facies found in Hole 639D represent deposition in an inner platform environment—more precisely in a deep lagoon—devoid of a filling sequence and far from any significant barrier. The nature and composition of the observed matrices also imply that this lagoon was in communication through a discontinuous barrier with the open sea, not affected by wave agitation but receiving some detrital input. In terms of margin paleogeography, such an arrangement corresponds to a gently sloping ramp (Ellis, 1984; Read, 1985; Gawthorpe, 1986; Wright, 1986).

An alternative hypothesis involving an outer platform environment, devoid of a barrier, leads to the same concept of a

Figure 7. Wackestone with gastropods. Dominantly micritic matrix contains a significant amount of gastropods and a few oncoids, as well as large foraminifers. Sample 103-639D-6R-3, 31-36 cm (negative print from thin section, 6.5X).

ramp. In this case, distinction between outer and inner environments is purposeless. Hole 639D was located on this ramp, the size and polarity of which are unknown because the data come from a single drill hole. However, analysis of the microfacies succession allows us to reconstruct the chronological evolution of the ramp as well as to distinguish relations existing between biological and depositional environments.

Paleoenvironmental Interpretation of the Microfacies Association and Succession

The development of the ramp sequence postulated at Hole 639D is reconstructed as follows:

Alternation of Oncoid- and Mollusk/Foraminifer-Bearing Units (Lower Part of the Limestone Sequence; Cores 103-639D-13R to 103-639D-9R)

Indications of Open Marine and Quiet Environments

Small agglutinated benthic foraminifers, siliceous sponge spicules, rare calpionellids, and pelagic thin calcitic lamellibranchs occurring (particularly in subunit *b*) in micritic and micropackstone matrices are interpreted as indicating an open marine and quiet environment of deposition. Additional evidence for this interpretation includes the abundance of micropackstone matrices and the nature of their components (micropellets, tiny bioclastic micritized grains, and tiny bioclasts resulting from an extreme fragmentation), which suggest *in-situ* destructive biologic activity.

Large bioclasts and whole intact organisms, such as large foraminifers, lamellibranchs, gastropods, siliceous sponges, and algae (cf. Arnaud, 1981), are found together locally with their debris as products of *in-situ* disaggregation in the muddy matrices of subunits *b* and *d*. This assemblage is interpreted as consisting of *in-situ* faunas, living in quiet environments with the effects of an outer influence.

Indications of Moderate and Variable Energy Environments

Subunits *a*, *c*, and *e* (Fig. 11) evidence more dynamic environments, including (1) a decrease in the percentage of matrix, with dominant heterometric packstones and rare grainstones; (2) concentration of large benthic foraminifers, generally winnowed by bottom currents for a short distance from their original, quiet biotope (described in the preceding); (3) an increase in abraded bioclastic debris (*Trocholina*, lamellibranchs, etc.); and (4) the accumulation of oncoids, the significance of which is discussed in the following text.

Significance of Oncoids

Oncoids have been long considered as characteristic of inner platform environments. It is now thought that, as a result of some genetic convergence, they can be produced in such various environments as fluvial (Leinfelder, 1985), lagoonal (most authors), and under an outer influence, below the turbulent wave zone (Gaillard, 1983; Bernier, 1984). Thus, oncoids are not precise zonal markers of a platform environment but, rather, are an indication of hydrodynamic changes in a given environment (Carozzi et al., 1983).

The autochthonous nature of oncoids in subunits *a* and *c* (Fig. 11) is evidenced by (1) their good surficial preservation (*Nubecularia* chambers; cf. Pl. 2, Fig. 3), (2) the absence of broken specimens, and (3) the presence of quartz particles of similar size in both oncoids and sediment. The fact that nuclei are extracted from the sediment indicates minor transportation (from a slightly more agitated zone) of these elements into a globally quiet environment.

Minor variations in oncoid shape and structure are the result of hydrodynamic fluctuations. Irregular morphologies are produced during the low-energy periods (Purser and Loreau, 1973; Loreau, 1982), whereas concentrations of rounded, well-sorted oncoids, in association with composite grains or micritized and abraded bioclasts (the first variant of microfacies type 2) result from more intense hydrodynamic conditions, implying a necessary degree of energy for the generation of grapestones (Cros, 1979).

The observed bioturbation resulted in a mixing of two facies that initially differed by their hydrodynamic regimes. Thus, most of the packstones with oncoids and large foraminifers (microfacies type 1) represent mixing, through bioturbation, of two sediments. One component sediment was originally probably a wackestone with pelecypods and large foraminifers (microfacies type 4), reflective of periodically quiet bottom conditions. The other component sediment was composed of oncoids. The observation on a thin-section scale of the intermixing caused by bioturbation implies that these sediments were initially deposited in close proximity to each other and that, on a larger scale, they were synchronous, with numerous vertical and lateral interfingerings. Bioturbation also explains the observed recycling of oncoids and bioclasts, which serve as nuclei for larger oncoids (Figs. 3 and 5).

Relation of the Two Environments of Deposition

In summary, the analysis of various microfacies from the basal unit of Hole 639D reveals the existence of two distinct and synchronous environments for the deposition of carbonates. One environment of deposition, corresponding to the microfacies with mollusks, large foraminifers, and accessory algae, favored the development of sessile and mud-burrowing organisms and involved a stable and quiet, but bioturbated, environment. The other depositional environment was more complex. It corresponds to the oncoid-bearing facies, thereby suggesting a vari-

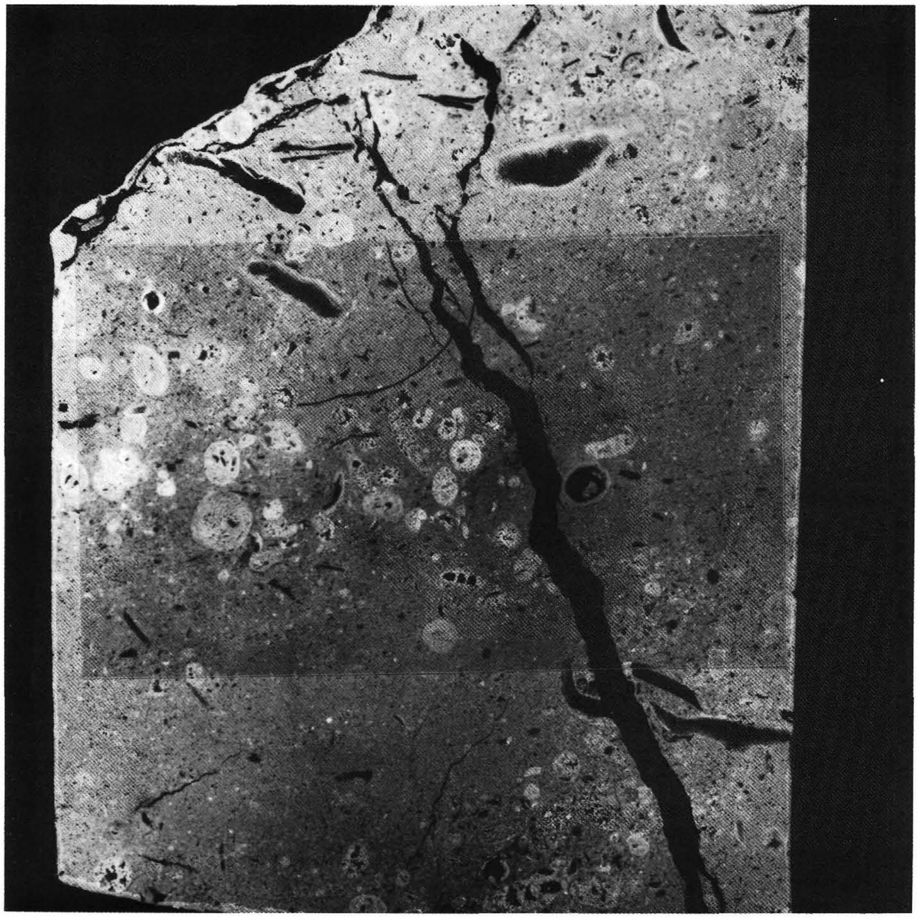

Figure 8. Mudstone to wackestone with large foraminifers; note the significant decrease of both oncoids and mollusk bioclasts in comparison with samples shown in Figs. 6 and 7. Sample 103-639D-6R-3, 30–34 cm (negative print from thin section, 6.5X).

able, but never turbulent, hydrodynamic regime. Intense bioturbation affected oncoid productivity by shortening the time needed for encrustation to develop and also disturbed the initial sedimentary record. Such an active environment differs from that defined for inner platform lagoons ("Comblanchian" upper Bathonian lagoon of Burgundy; Purser, 1975; cf. Peryt, 1983) but resembles those described for the Kimmeridgian outer platform zones of Jura (Bernier, 1985), the area surrounding the Oxfordian sponge reefs of Jura (Gaillard, 1983), and the lower Bathonian outer platform facies of Burgundy (Purser, 1975; P. Cros, unpubl. data).

Both of these two environmental types, resulting only from slight differences in bathymetry, occur under the same bottom conditions of a ramp. We assume that the more stable (hydrodynamically) areas were at slightly shallower depths than the oncoid-bearing zones, for they appear to be the source of nuclei for the latter (Fig. 12).

Detrital Influx Superimposed On and Mixed with Carbonate Deposits (Subunits f though i; Cores 103-639D-8R through the lower part of 103-639D-6R)

The sudden appearance of sandstones (subunit *f*) above the carbonate sequence (subunits *a* through *e*) might be the exaggerated result of the masking of possible transitional beds caused by insufficient core recovery. The same environmental conditions as those suggested for carbonate deposition seem to have persisted, as shown by the presence of the same bioclasts, oncoids, and matrices during the detrital episode. Thus, this detrital influx has no intrinsic value in distinguishing the proximity of the littoral zone. The bracketing of the sandy subunit *f* by two oncoid-bearing subunits (*e* and *g*) is representative of a channeling terrigenous transit conveyed into deeper and more agitated carbonate depositional zones during a time of higher hydrodynamic activity.

In the environment that produced oncoid-bearing deposits, the mixing of siliciclastics and carbonates led either to alternating coarse sandstones and bioclastic limestones of various grain sizes (subunit *h*) or to an intricate deposit of fine- to medium-grained quartz particles and oncoids in various stages of growth (subunit *g*). These two modes of mixing suggest two different hydrodynamic levels and that a dominant role was played by currents. Subunit *g* is topped by a mudstone, an indication of a quiet environment.

In a context of alternating or mixed clay/carbonate beds, devoid of oncoids, the terrigenous deposits of subunit *h* represent all energy levels of depositional mechanisms, up to the stage of clay decantation. This second detrital impulse starts with a silty clay decantation, consistent with the energy level of the carbonate environment. An increasing energy level is depicted by the upward succession of the recovered facies, with alternating detrital deposits and bioclastic facies containing mollusks and large foraminifers. The hydrodynamic conditions of the terrigenous deposits and interbedded or intermixed carbonates appear to be in good agreement.

Subunit *i* is characterized by (1) a dominant heterometric wackestone texture, (2) an almost complete disappearance of

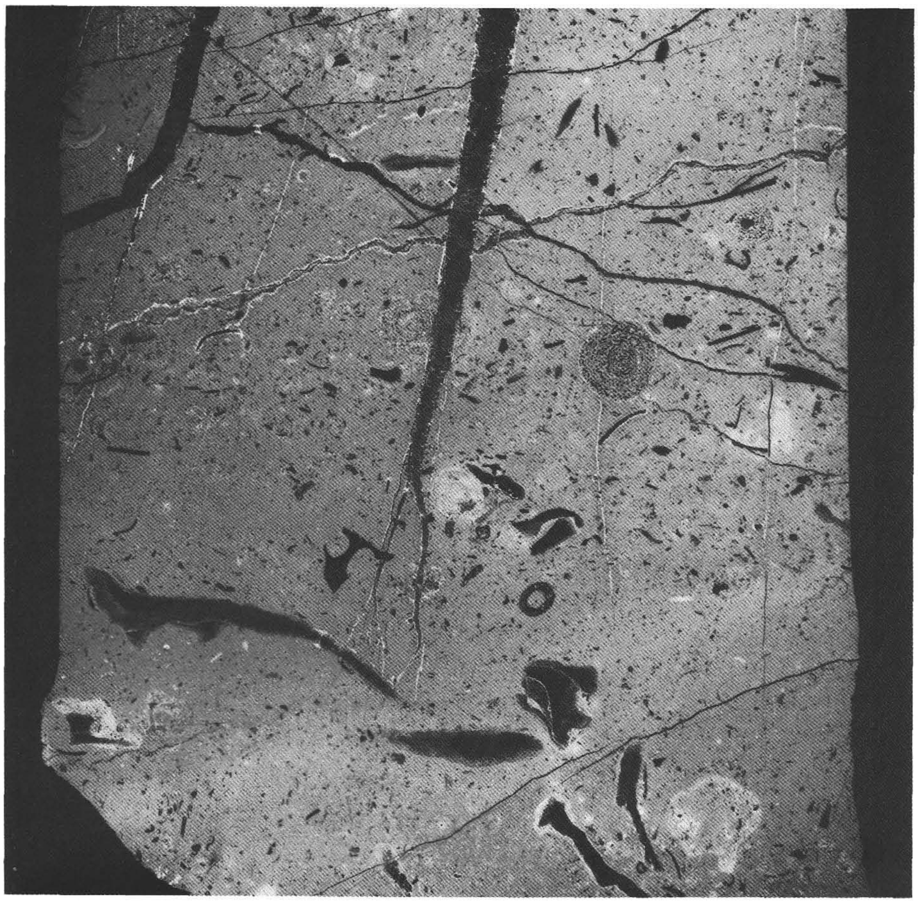

Figure 9. Wackestone-floatstone with pelecypods and large foraminifers. Matrix is strictly micritic or clotted and rich in bioclastic microdebris. Dominant allochems are fragments of calcite, fibrous pelecypods, and large foraminifers. Sample 103-639D-10R-1, 39–42 cm (negative print from thin section, 6.5X).

terrigenous influx, (3) decrease in the dominance of oncoids, and (4) the dominance of large foraminifers and molluscan and algal debris. This subunit was thus deposited in an initially low-energy hydrodynamic regime that was sufficiently strong to favor oncoid generation. This regime was succeeded by a quieter environment that favored the formation of molluscan (in particular gastropods)/foraminiferal assemblages and also possibly (although not fossilized) marine grasses.

Recurrence of a Quiet Environment Devoid of Coarse Terrigenous Influx (Subunit j; Upper Part of Core 103-639D-6R).

Subunit *j* includes mudstones in its lower part, which suggests an extremely quiet environment that would have been less favorable for bottom-dwelling organisms. Oncoids are absent or rare as components, superseded by irregular and incomplete encrustations on unabraded, identifiable, and untransported bioclastic elements (mostly foraminifers, bryozoans, and serpulids). Algal debris are also more abundant and of greater size (up to 200 μm) than in the underlying subunits.

These features, in addition to the texture and micropackstone matrices, do not imply any bathymetric increase but only evidence a recurrence of stable muddy bottoms.

Significance of Floatstones with Small Coral and Sponge Debris (Subunit k; Cores 103-639D-5R and 103-639D-4R)

The microfacies of subunit *k* is characterized by marked changes in comparison with the underlying subunits. These differences include: (1) the concomitant presence (in variable percentages) of millimeter to centimeter size corals and Pharetrone and Chaetetid sponges (some in life position; Pls. 6 and 9) as dominant components; (2) the disappearance of oncoids and a strong reduction in the abundance of large foraminifers (with the exception of a few basal layers, e.g., Sample 103-639D-5R-3, 13–16 cm); (3) encrustations developed on large bioclastic debris; (4) the rarity of micropackstone texture matrices, with heterometric wackestone or floatstone as the dominant texture; and (5) the observation of evidence of synsedimentary lithification (Loreau and Cros, this volume).

These characteristics of subunit *k* point to a significant change. The environment of deposition became quiet and uniform, with a stable bottom inhabited by small individuals and colonies of corals, various calcareous sponges, numerous pelecypods, and echinoderms. Large foraminifers and algae are scarce or even absent in subunit *k*. The increase in the abundance of siliceous sponges, mutually exclusive of coral buildups (Fischer, 1969), must be emphasized. However, this association is not unusual (Fischer, 1969; Gaillard, 1983). The composition of the assemblages, the small (normal) size of corals, the presence of genera and growth modes known to be related to muddy environments (Gill and Loreau, this volume), and their occurrence as broken and encrusted pieces are not characteristic of biohermal or biostromal facies. Rather, these characteristics suggest deeper and stable muddy bottoms, not far from "coralligenous bottoms" with a bathymetry of 50–70 m described by Perès and Picard (1964).

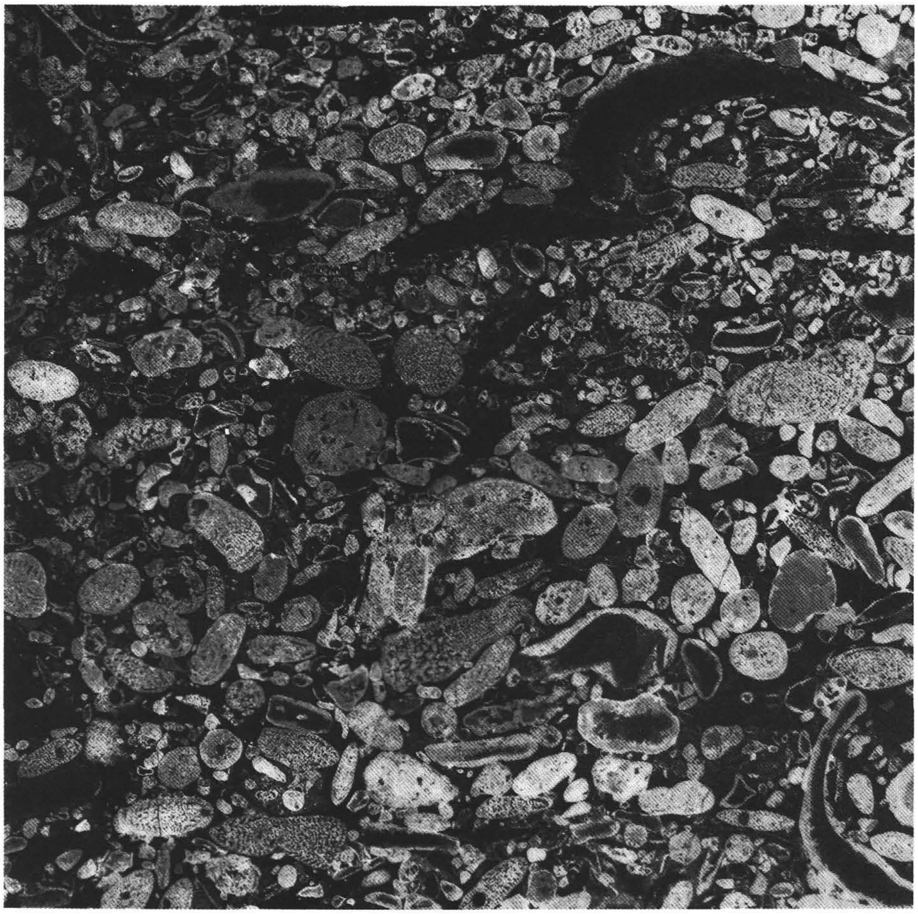

Figure 10. Heterometric bioclastic grainstone with large foraminifers (dominantly *Anchispirocyclina*), recrystallized pelecypods, and algal fragments. The smaller grains are worn and micritized, similar to pellets. Sample 103-639D-7R-1, 71–75 cm (negative print from thin section, 6.5X).

According to logging data (Shipboard Scientific Party, 1987), subunit *k* includes a detrital layer about 1 m thick (not recovered by drilling) that consists of silty clay, calcareous silt, and marl. This bed overlies a sequence of mudstone and micropackstone enriched with calpionellids, thin pelecypod shells, small benthic foraminifers, sponge spicules, and calcispheres, all of which indicate a quiet, open environment, evocative of basinal conditions. Again, the detrital influx is only superimposed on a given environment.

We also note that subunit *k* also contains at least two zones consisting of micritized and reworked bioclasts (Samples 103-639D-5R-3, 13–16 cm, and 103-639D-4R-1, 11–13 cm), which suggests some resedimentation from a shallower, more turbulent area.

These features of subunit *k* are consistent with our general interpretation of a euphotic and relatively deep ramp during the late Tithonian for the area drilled at Hole 639D.

Initial Nature and Environment of the Dolomitic Limestones (Subunit l; Cores 103-639D-3R and 103-639D-2R)

The stratigraphic position and tectonic or morphologic significance of dolomites recovered in most of the Site 639 holes (Holes 639B–639F) remain unclear or at least questionable. Only in Hole 639A is the dolomite immediately overlain (through an unconformity) by lower Valanginian marls and thus, is its stratigraphic position known. Dolomite from all of the Site 639 holes shows various crystalline textures that confuse identification of the initial texture and composition. However, a sufficient number of bioclast ghosts (mainly echinoderms, plus rare pelecypods, algae, Pharetrone sponges, corals, and very rare *Anchispirocyclina* fragments) are identifiable in some Hole 639D dolomitic microfacies to suggest that the initial microfacies was not fundamentally different from the floatstone with corals or bioclastic heterometric packstone types. No features related to peritidal environments are recognizable (Loreau and Cros, this volume).

CONCLUSIONS

Because of relatively poor core recovery, uncertainty about the thickness of the formation, and analysis of samples from only one hole, the interpretation of the limestone succession recovered at Hole 639D is not well constrained. However, it is possible to propose a model for the deposition of the facies based on Walther's classical law of vertical and lateral facies changes.

There is no evidence in this sequence of either typical lagoonal (no peritidal confined facies) or barrier (no bioclastic or oolitic sands) deposits that would suggest a succession of platform facies and allow their interpretation in terms of platform zonation. Rather, the depositional environment could have been an open, but not too shallow, area that received periodic terrigenous input and was not influenced by a remote reefal barrier. On an open shelf, this corresponds to the lower infralittoral zone, from 30 to 60–70 m water depth. Deposition is influenced by the gentle slope of this environment, commonly labeled as a carbonate ramp.

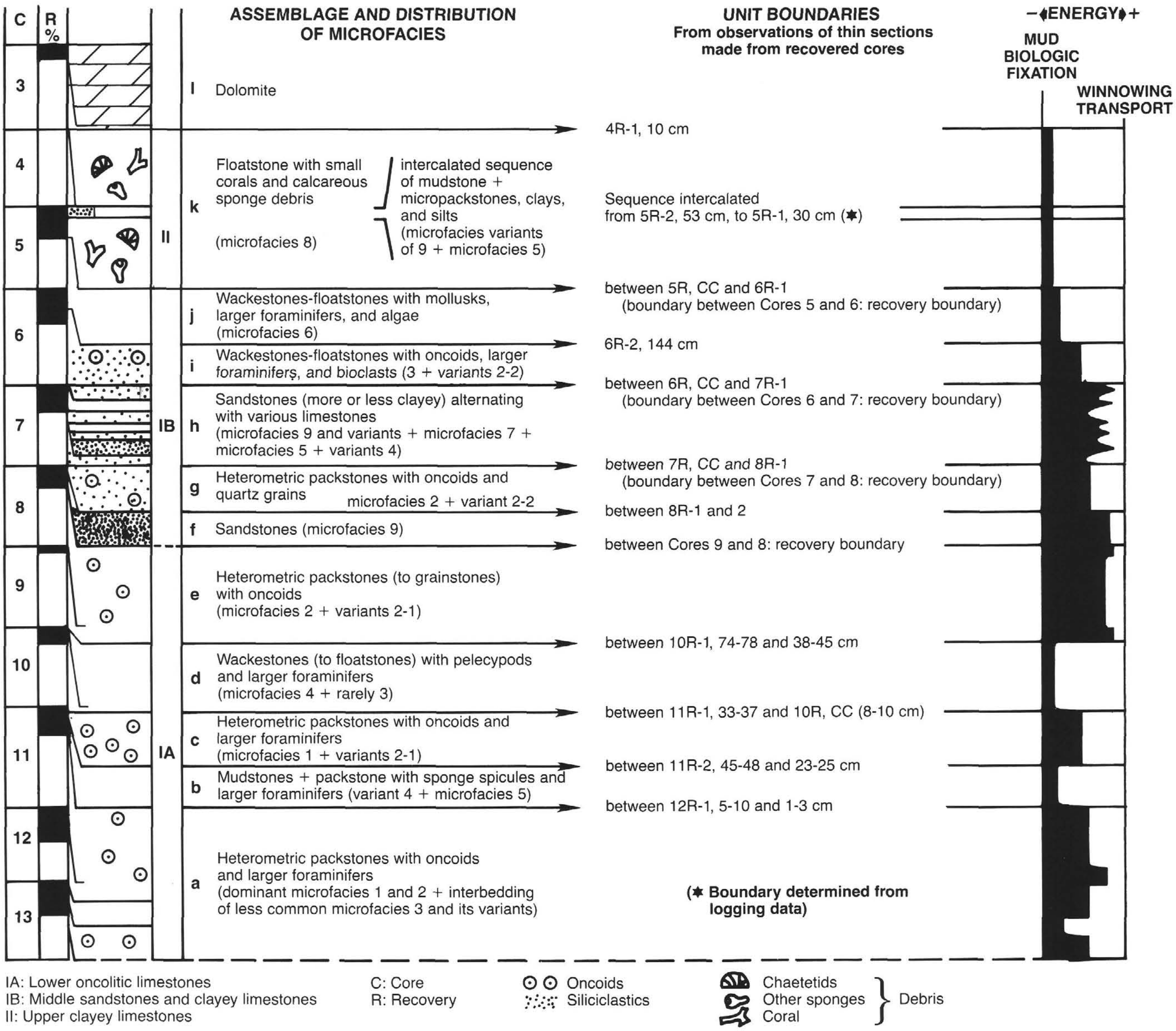

Figure 11. Subunits based on microfacies, Hole 639D.

The distribution of three dominant microfacies (types 1, 2, and 4) indicates that the morphostructure of the ramp was characterized by a slightly variable bottom stability during its early evolution. Three local environments influenced bottom deposition and life (Fig. 12).

1. Stable muddy areas favored the growth of benthic faunas and floras, including mollusks, various benthic foraminifers, siliceous sponges, and calcareous algae (mainly small and delicate chlorophycaean thalli). Active formation of small pellets by unidentified deposit feeders and the accumulation of fine bioclastic debris further characterize this quiet environment. The stable and bioturbated areas were probably a little shallower than the rest of the ramp, if we consider the trapping and binding action of the fine sediments.

2. A bottom with weak turbulence evolved from the preceding quiet, muddy environment. Deposition of coarse bioclastic grains was not sorted, but fine-grained particles were removed by winnowing. Occasional periods of bottom stability alternated with periods of slight reworking of bioclasts, resulting in the coating of grains. This alternation of coating processes with the bioturbation of sediments containing bioclasts and oncoids resulted in irregular textural variations and limited the coating thickness of the grains.

3. Surrounding the preceding interrelated environments were deeper bottom areas with moderately turbulent conditions that favored the concentration of coarse bioclastics and the accumulation of sediments rich in rounded and generally sorted oncoids. Composite grains with oncoids resulted from the alternation of quiet and turbulent conditions during the periods of reworking.

The superimposed siliciclastic deposits (microfacies type 9) were probably transported in channels that correspond to the regions of greatest water depth. Their mixing with calcareous sediments occurs laterally (microfacies type 2 variety of packstone with oncoids, foraminifers, and fine quartz grains); the sand-sized grains are associated mainly with oncoid accumulations

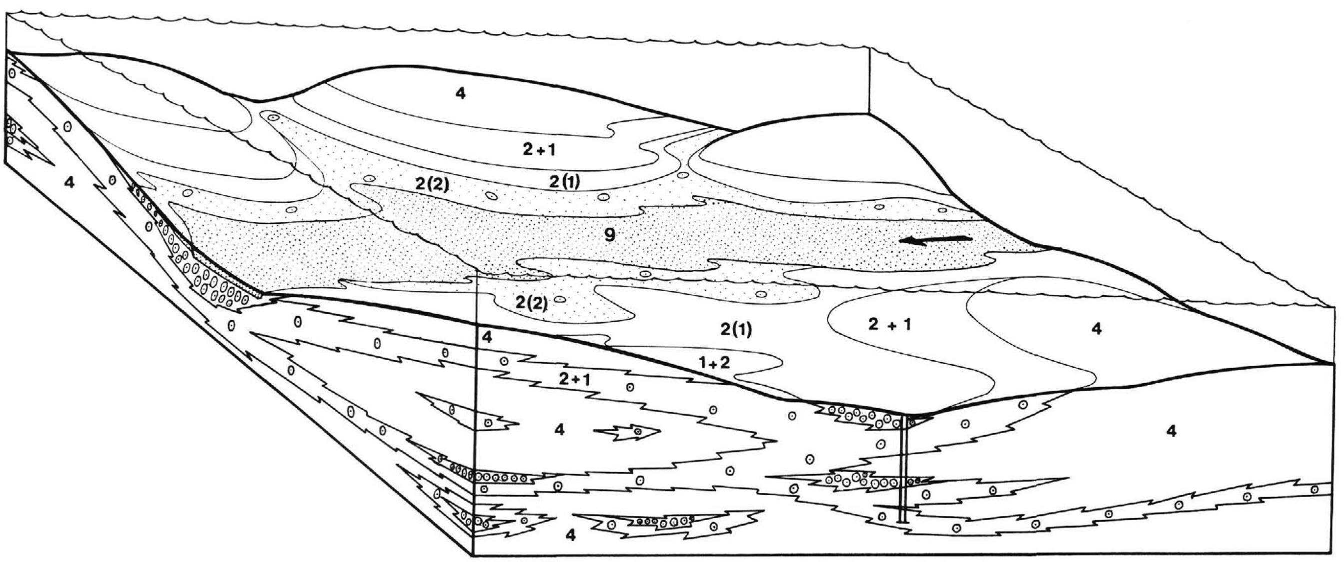

Figure 12. Tentative schematic reconstruction of the late Tithonian sedimentary environment of Hole 639D, showing a ramp with mixed carbonate and terrigenous deposits. The area covered is some square kilometers; height is greatly exaggerated. The suggested scheme corresponds to the paleoenvironmental interpretation of Cores 103-639D-13R through 103-639D-8R. The microfacies type numbers are described in the text.

whereas the silt-sized grains are usually linked with the oncoid-coating milieu. These mixed bottoms suggest a hydrodynamic analogy between the "turbulent" zones with oncoids and the sandy terrigenous zones.

During the second evolutionary stage of the ramp, the alternating oncoid-rich and stable bottoms were replaced by an essentially stable muddy bioclastic bottom, where fixed calcareous organisms such as corals, calcareous sponges (Pharetrones and Chaetetids), and siliceous sponges dwelled. As a rule, the biogenous primary structures are small and fragile; some are reworked and irregularly coated by various encrusting organisms. This assemblage of organisms, which is known to live in muddy environments, does not correspond to a reef or a reef slope, suggesting instead a stable bottom with binding organisms. This combination is usually mutually exclusive, and neither corals nor siliceous sponges were able to grow continuously.

This stage is comparable to an ephemeral and aborted evolution of the "mud mound" type, the development of which is well known in the middle and outer ramp areas (Gawthorpe, 1986; Wright, 1986). A slight increase in water depth up to 60 or 70 m and a stronger open-sea influence are implied by this situation. Corroboration is provided by the small increase in the abundance of calpionellids and a significant decrease in the number of large benthic foraminifers in the upper subunit *k* (Fig. 2).

Similar facies (containing Anchispirocyclines, Trocholines, pelecypods, corals, algae, calpionellids, oncoids, detrital influxes, etc.) have been described from the Upper Jurassic in several areas along the Portuguese continental margin, particularly in eastern Algarve (Durand-Delga and Rey, 1982; Ramalho, 1985). Less similar sequences were described in the Lusitanian Basin (Ellis, 1984). We are tempted to reinterpret the sequence described in Algarve as indicative of an open shelf (carbonate ramp) rather than a wide confined lagoon, as suggested by Ramalho (1985). On the other hand, Ellis (1984) also suggested the concept of a ramp for the environment of deposition of the "Calcaires de Mem Martins," deposited during the Kimmeridgian in the Lusitanian Basin.

ACKNOWLEDGMENTS

M. Moullade, J.-P. Loreau, and J. Thurow wish to thank the Ocean Drilling Program for inviting them to participate on Leg 103 aboard the *JOIDES Resolution*. The authors extend their thanks to A. W. Meyer, T. Steiger, J. P. Weight, and J. C. Fischer for their comments. This work was supported by French C.N.R.S. Grant "ATP Géologie-Géophysique des Oceans" no. 1243, 981037 and 981059.

REFERENCES

Arnaud, H., 1981. De la plate-forme urgonienne au bassin vocontien: le Barrémo-Bédoulien des Alpes occidentales entre Isère et Buëch (Vercors méridional, Diois oriental et Dévoluy). *Geol. Alp.*, 12:1–804.

Bernier, P., 1984. Les formations carbonatées du Kimméridgien et du Portlandien dans le Jura Méridional. Stratigraphie, micropaléontologie, sédimentologie. *Doc. Lab. Geol. Fac. Sci. Lyon*, 92:1–730.

Carozzi, A. V., Falkensheim, F.U.H., and Franke, M. R., 1983. Depositional environment, diagenesis and reservoir properties of oncolitic packstones, Macae Formation (Albian-Cenomanian), Campos Basin, offshore Rio de Janeiro, Brazil. *In* Peryt, T. (Ed.), *Coated Grains*: Berlin (Springer Verlag), 330–343.

Cros, P., 1979. Genèse d'oolithes et de grapestones, plate-forme des Bahamas (Joulters Cays, Grand Banc). *Bull. Cent. Rech. Explor. Prod. Elf Aquitaine*, 3:63–139.

Cuif, J. P., Feuillée, P., Fischer, J. C., and Pascal, A., 1973. Présence d'astrorhizes chez les Chaetetida mésozoiques. *C. R. Acad. Sci. Ser. 2*, 277:2473–2476.

Dunham, R. J., 1962. Classification of carbonate rocks according to depositional texture. *In* Ham, W. E. (Ed.), *Classification of Carbonate Rocks*: AAPG Mem., 1:108–121.

Durand-Delga, M., and Rey, J., 1982. Découverte de Calpionelles dans le Jurassique terminal et le Crétacé basal de l'Algarve (Portugal). *C. R. Acad. Sci. Ser. 2*, 295:237–242.

Ellis, P. M., 1984. Upper Jurassic carbonates from the Lusitanian Basin, Portugal, and their subsurface counterpart in the Nova Scotian shelf [Ph.D. thesis]. Open Univ., Milton Keynes.

Embrie, A. F., and Klovan, J. F., 1971. A late Devonian reef tract on northeastern Banc Islands, Northwest Territories. *Bull. Can. Pet. Geol.*, 19:730–781.

Fischer, J. C., 1969. Géologie, paléontologie et paléoécologie du Bathonien du sud-ouest du Massif Ardennais. *Mem. Mus. Nat. Hist. Nat. Ser. C (Paris)*, 20.

________, 1970. Révision et essai de classification des Chaetetida (Cnidaria) post-paléozoiques. *Ann. Paleontol.*, 56:149–233.

Fritz, G. K., 1958. Schwammstotzen, Tuberolithe und Schatlbrecien im Weissen Jura der Schwäbischen Alb. *Arb. Inst. Geol. Palaeontol. Univ. Stuttgart*, 13.

Gaillard, C., 1983. Les biohermes à sponglaires et leur environnement dans l'Oxfordien du Jura méridional. *Doc. Lab. Geol. Fac. Sci. Lyon*, 90:1–515.

Gawthorpe, R. L., 1986. Sedimentation during carbonate ramp to slope evolution in a tectonically active area: Bowland Basin (Dinantian), Northern England. *Sedimentology*, 33:185–206.

Leinfeider, R. H., 1985. Cyanophyte calcification morphotypes and depositional environment (Alenquer Oncolite, upper Kimmeridgian?, Portugal). *Facies*, 12:253–274.

Loreau, J.-P., 1982. Sédiments aragonitiques et leur genèse. *Mem. Mus. Nat. Hist. Nat. Ser. C (Paris)*, 47.

Lucas, G., Cros, P., and Lang, J., 1976. *Etude Microscopique des Roches Meubles et Consolidées*: Paris (Doin).

Perés, J. M., and Picard, J., 1964. Nouvean manuel de bionomie benthique de la Mer Méditerranée. *Bull. Rec. Trav. Stat. Mar. Endoume*, 47.

Peryt, T. (Ed.), 1983. *Coated Grains*: Berlin (Springer-Verlag).

Purser, B. H., 1975. Sedimentation et diagenèse précoce des séries carbonatées du Jurassique moyen de Bourgogne [Thesis]. Univ. Orsay.

Purser, B. H., and Loreau, J.-P., 1973. Aragonitic, supratidal encrustations on the Trucial Coast, Persian Gulf. *In* Purser, B. H. (Ed.), *The Persian Gulf*: Berlin (Springer Verlag), 343–376.

Ramalho, M., 1985. Considérations sur la biostratigraphie du Jurassique supérieur de l'Algarve oriental (Portugal). *Comun. Serv. Geol. Port.*, 71:41–50.

Read, J. F., 1985. Carbonate platform facies models. *AAPG Bull.*, 69: 1–21.

Shipboard Scientific Party, 1987. Site 639. *In* Boillot, G., Winterer, E. L., et al., *Proc. ODP, Init. Repts.*, 103: College Station, TX (Ocean Drilling Program), 409–532.

Wright, P. V., 1986. Facies sequences on a carbonate ramp: the carboniferous limestone of South Wales. *Sedimentology*, 33:221–241.

Date of initial receipt: 27 March 1987
Date of acceptance: 20 October 1987
Ms 103B-149

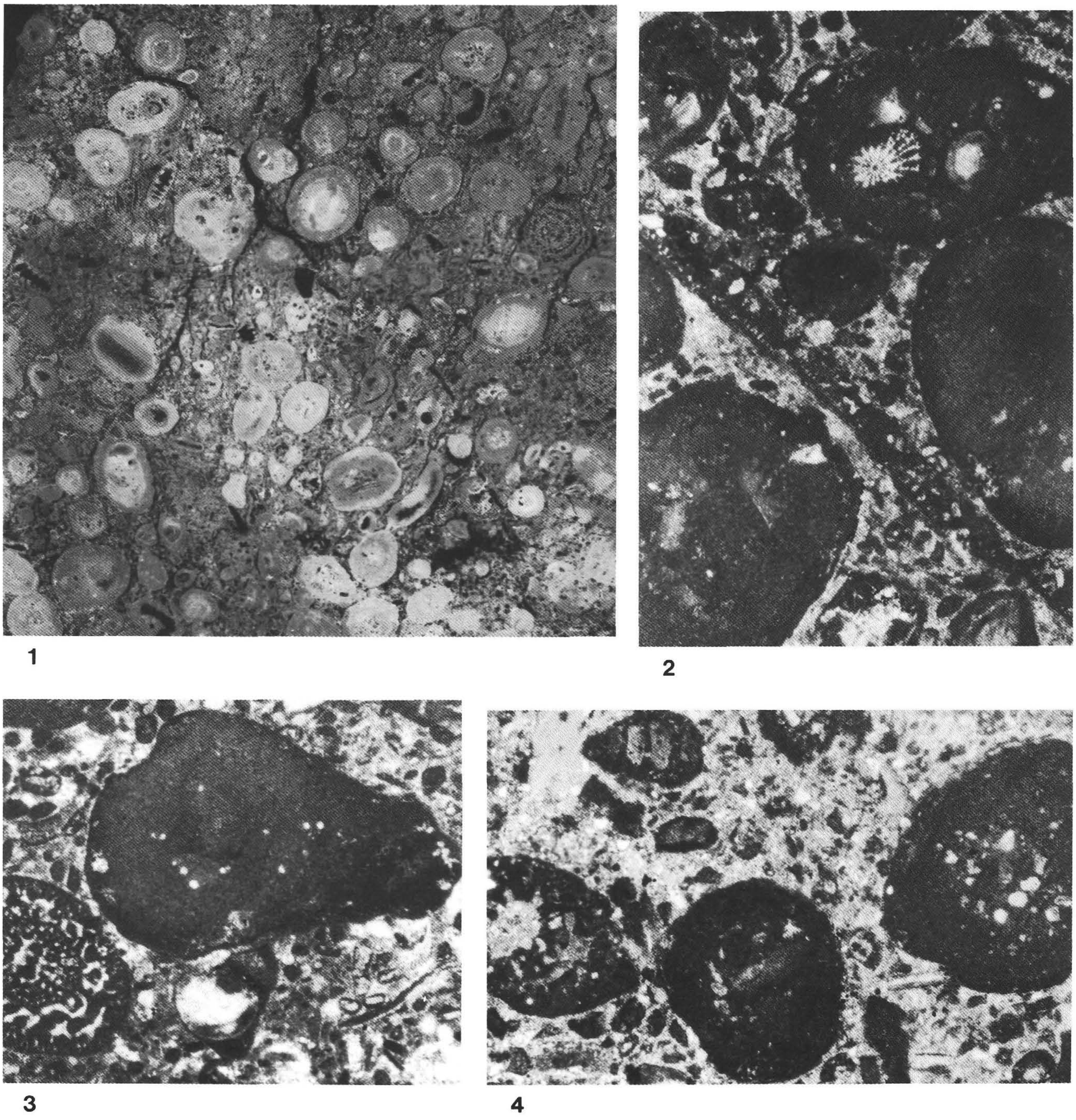

Plate 1. **1.** Negative prints from thin sections. Heterometric packstone with oncoids and associated grapestones. Sample 103-639D-11R-1, 142–144 cm (6.5X). **2.** Micritic-coated oncoids, each consisting of a composite nucleus and an external nubecularian coating. Matrix is the micropackstone type with *Thaumatoporella*. Sample 103-639D-11R-1, 146–149 cm (33X). **3.** Micritized and perforate composite grain; cavities are secondarily filled with sparite. Sample 103-639D-11R-1, 146–149 cm (28X). **4.** Silt-sized quartz grains present in the matrix, the cortex of oncoids, and the walls of agglutinated foraminifers. Sample 103-639D-8R-1, 130–133 cm (28X).

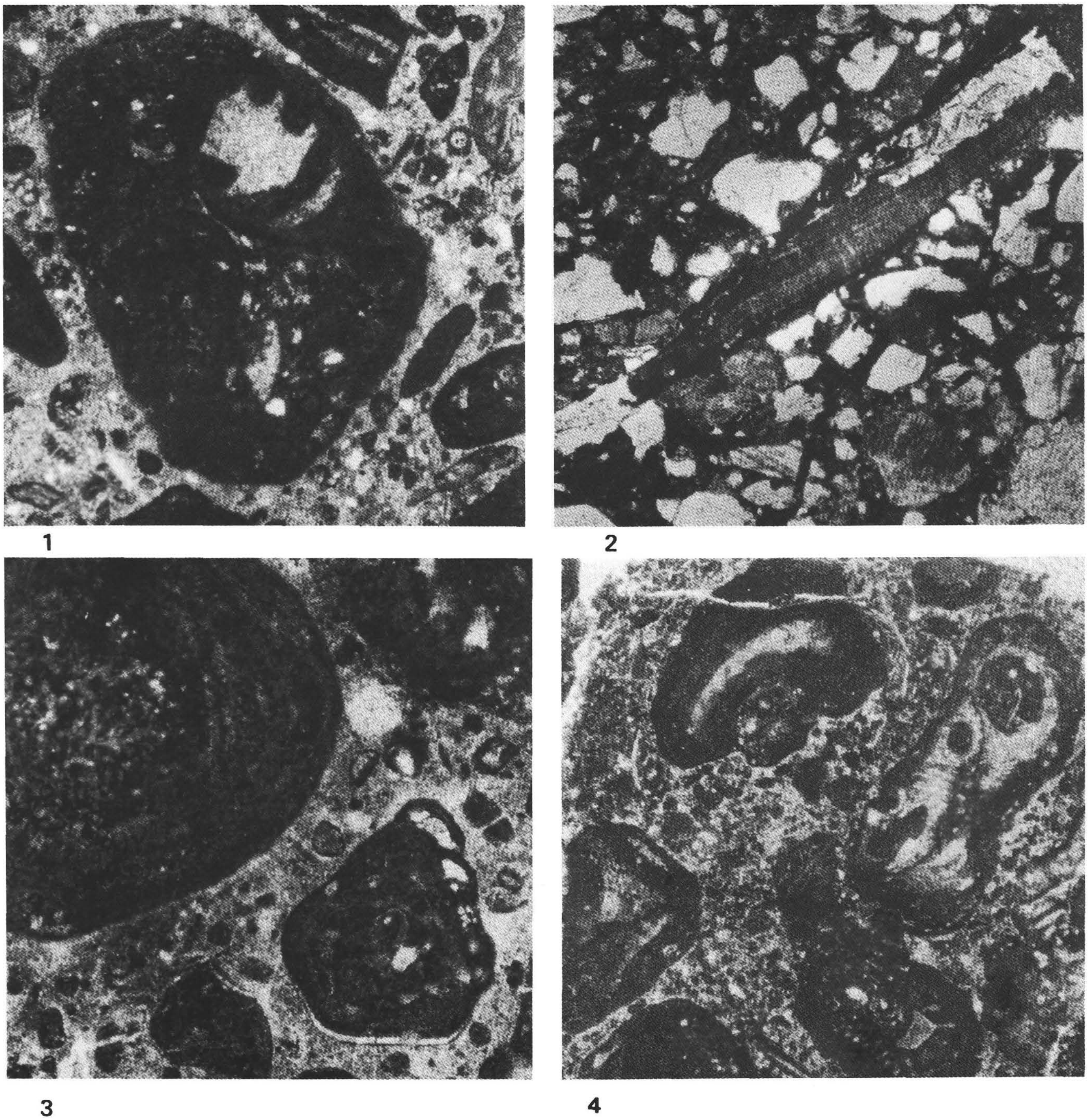

Plate 2. Negative prints from thin sections. **1.** Detail of a composite grain, including *Trocholina* and quartz, in a micropackstone matrix. Sample 103-639D-8R-1, 130–133 cm (38X). **2.** Sandstone with a clayey micritic matrix. Quartz grains are angular. The pelecypod shell fragment is partly silicified at both ends. Samples 103-639D-7R-2, 57–61 cm (25X). **3.** Detail of oncoids with a well-defined nubecularian coating; one of them is subrounded and shows a faintly laminated micritic cortex of algal(?) origin. Sample 103-639D-13R-2, 51–55 cm (60X). **4.** Irregular oncoids with various nuclei, including serpulids and pelecypod shells. Sample 103-639D-12R-3, 67–71 cm (25X).

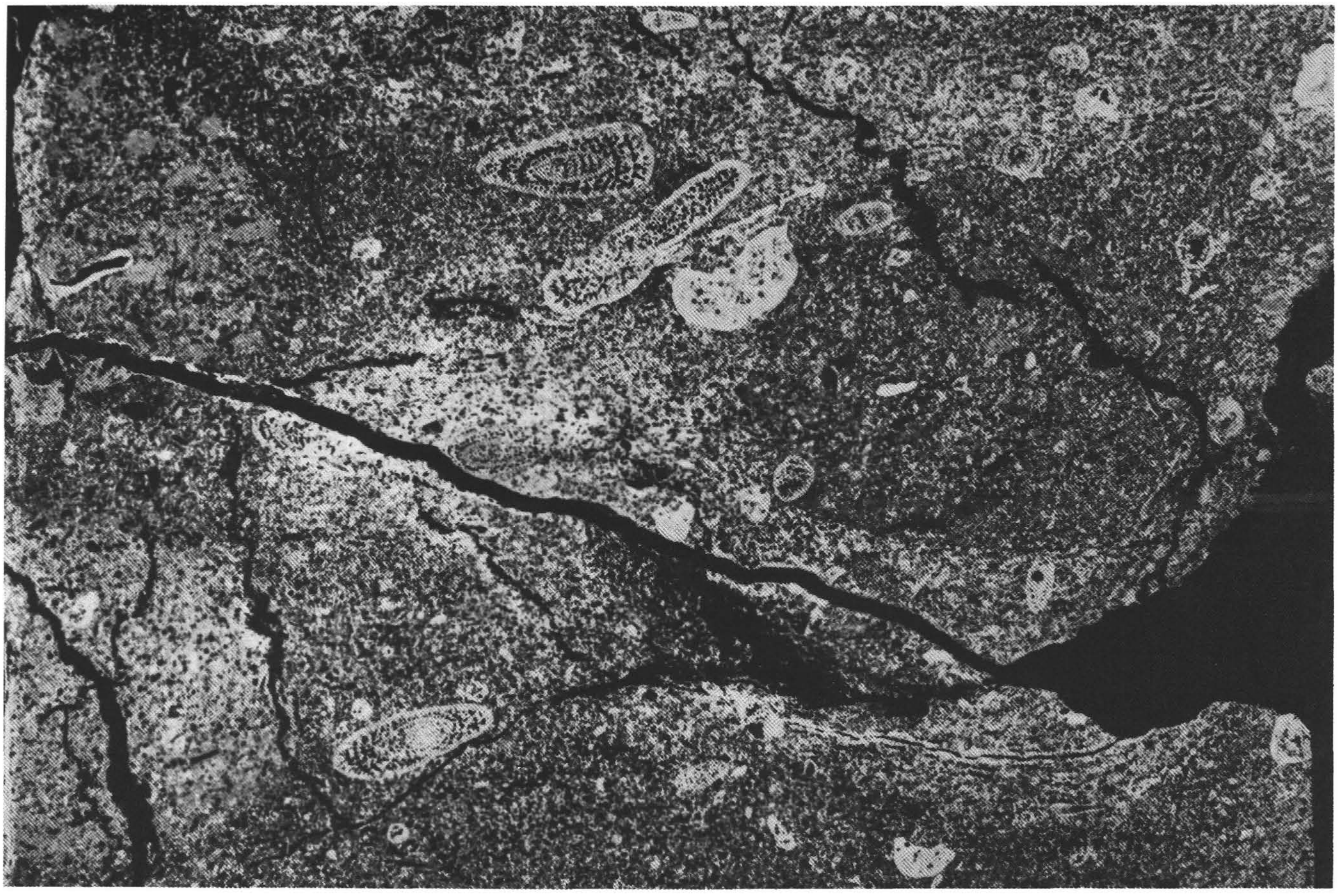

1

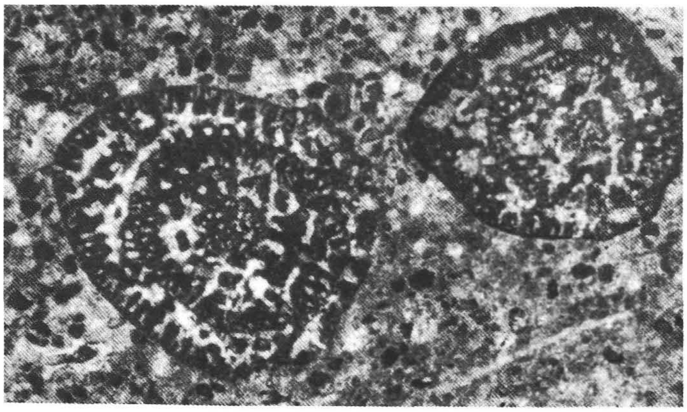

2

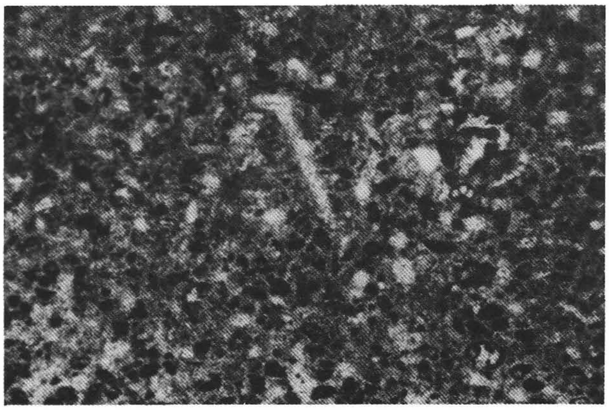

3

Plate 3. **1.** Matrix with a micropackstone texture, composed of micritic pellets of various origins. *Anchispirocyclina lusitanica* and rare oncoids are scattered. Sample 103-639D-11R-2, 45–48 cm (8X). **2 and 3.** Details of Figure 1 microfacies that better illustrate the matrix, oblique sections of *Anchispirocyclina* (Fig. 2), and a calcitized siliceous sponge spicule (Fig. 3) (28X).

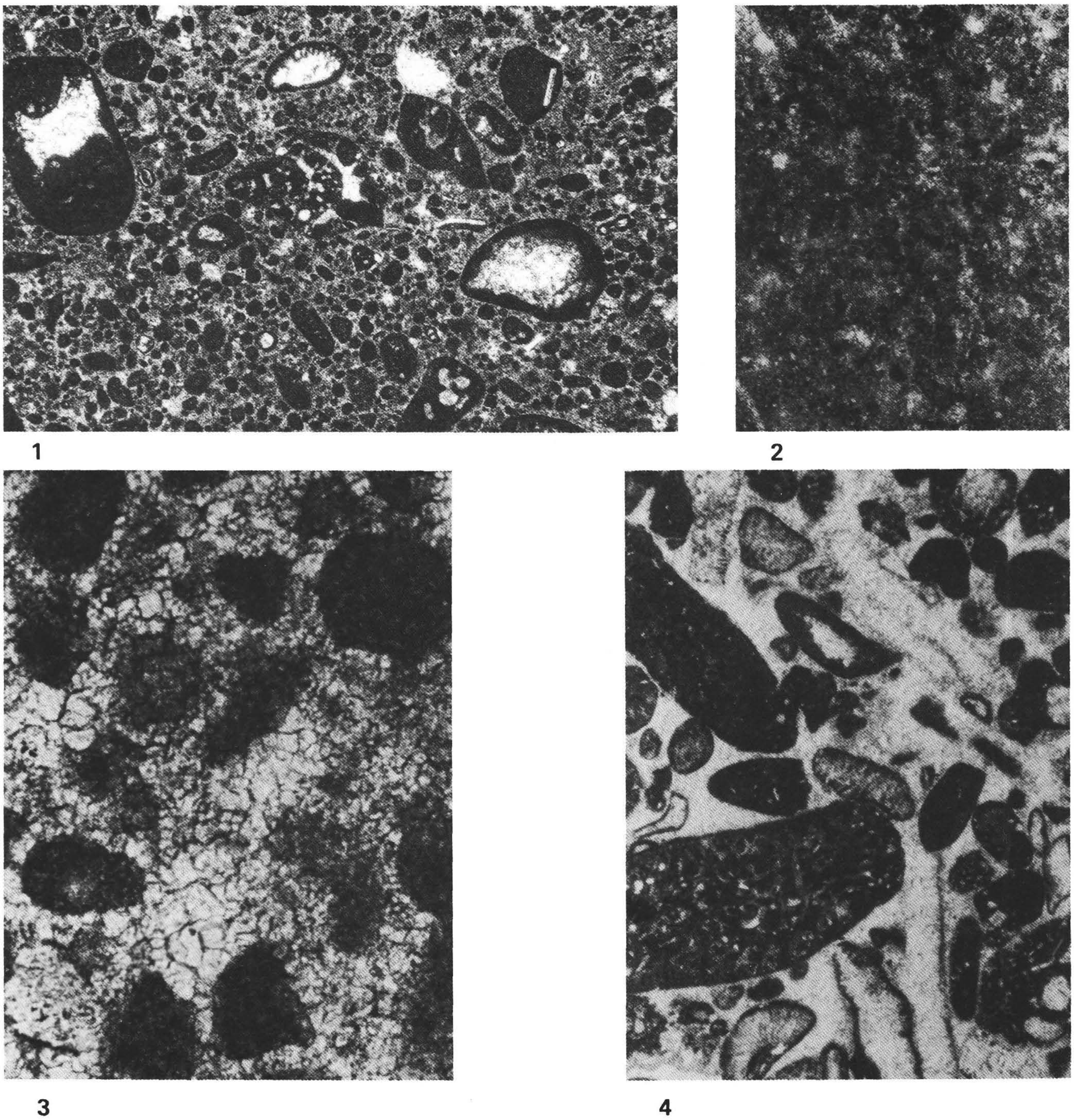

Plate 4. **1.** Heterometric packstone with oncoids and large foraminifers. Oncoids show a thin micritized cortex that is difficult to separate from the micritized nucleus. Sample 103-639D-13R-1, 77–80 cm (33X). **2.** Clotted structure of diagenetic origin. Sample 103-639D-5R-1, 134–136 cm (60X). **3.** Detail of a micropackstone texture matrix showing recrystallization of micrite and variably shaped micropellets. Sample 103-639D-11R-2, 45–48 cm (250X). **4.** Heterometric bioclastic grainstone, showing a detail of the microfacies in Figure 10, with varying degrees of micritization (which can lead to the development of pelletoids) and recrystallization of bioclastic debris (pelecypods and algae). Sample 103-639D-7R-1, 71–75 cm (33X).

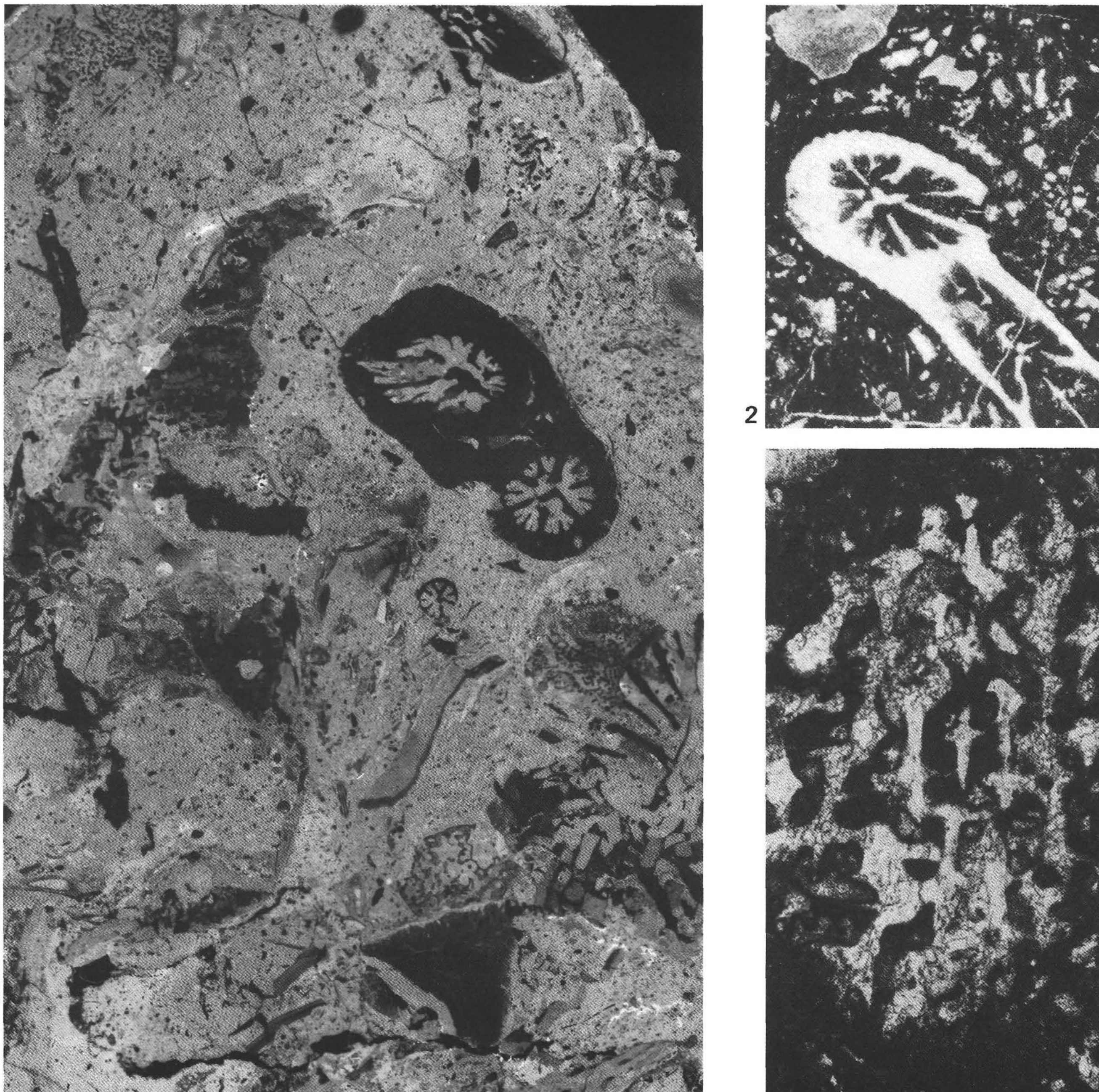

1 2 3

Plate 5. **1.** Floatstone with small corals and calcareous sponge debris. Biomicritic matrix is rich in small benthic foraminifers, sponge spicules, and a few Calpionellids. Sample 103-639D-4R, CC (7–9 cm) (Negative print from thin section. 6.5X). **2.** Coral fragment in a fine-grained bioclastic micropackstone matrix. Sample 103-639D-4R-2, 97–99 cm (12X). **3.** Typical pennulate structure of an encrusted coral fragment. Sample 103-639D-5R-3, 42–44 cm (30X).

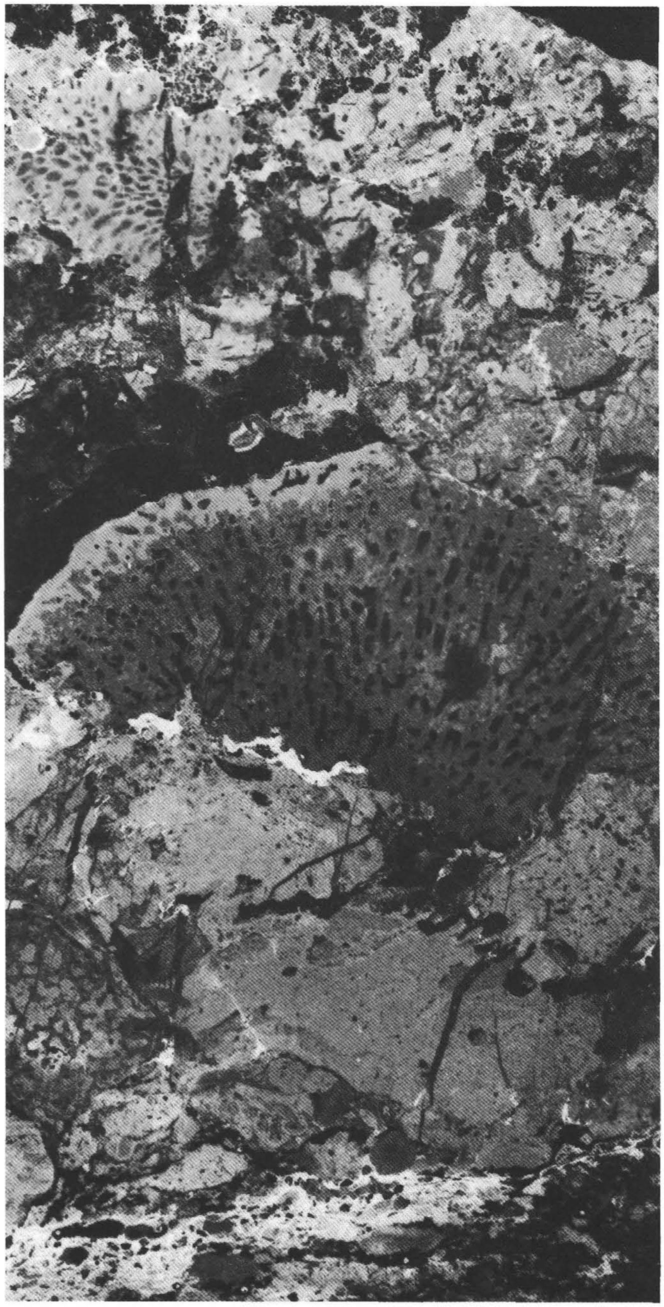

1

2

Plate 6. Negative prints from thin sections (6.5X). **1.** Floatstone with calcareous sponge debris (especially Chaetetids). Sample 103-639D-5R-2, 82–85 cm. **2.** Chaetetid microstructure showing delicate fibrous walls and sparitic infillings; included patches are siliceous. Sample 103-639D-5R-3, 39–41 cm.

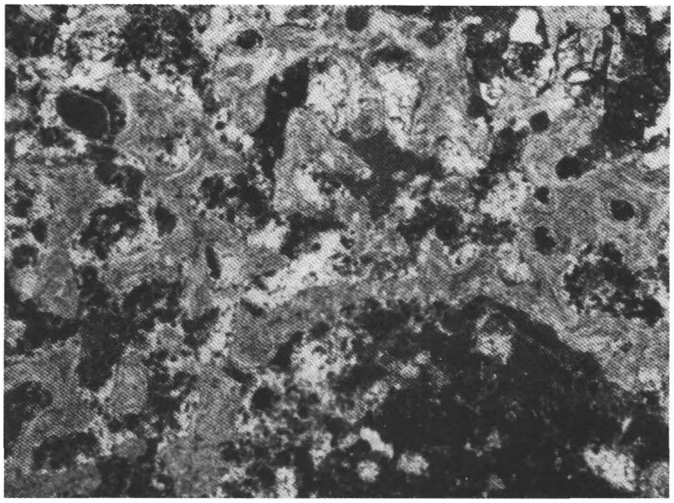

1

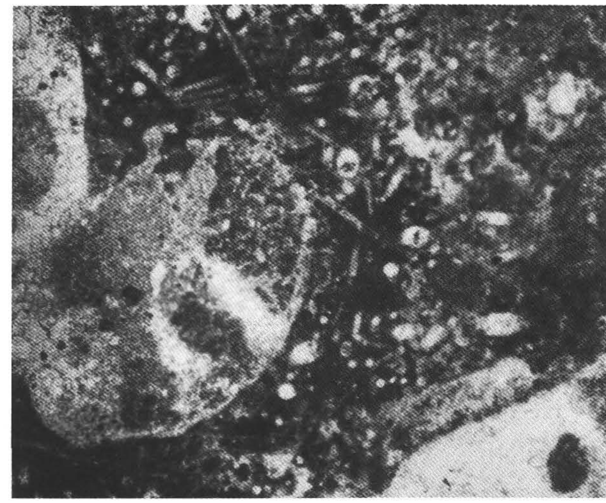

3

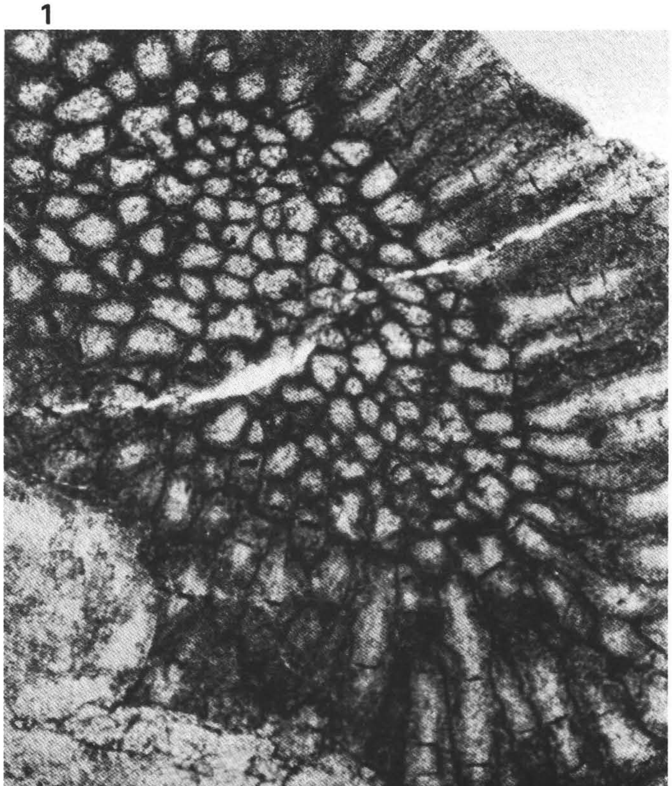

2

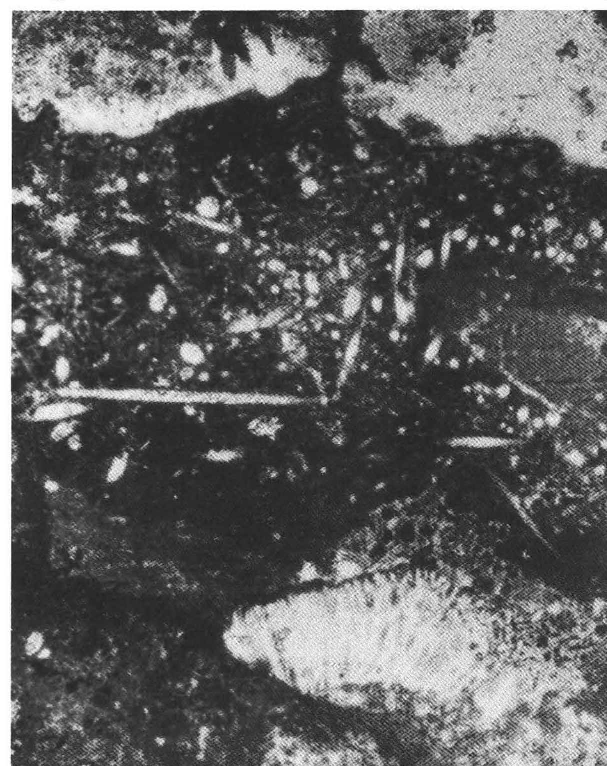

4

Plate 7. (30X). **1.** Pharetrone (calcareous sponge) fragment with the meandering canal structure filled by micrite and the well-preserved wall microstructure including monocrystalline flexuous spicules. Sample 103-639D-5R-2, 63–65 cm. **2.** Chaetetid microstructure with dark, fine fibrous walls and sparitic fillings. Sample 103-639D-5R-3, 39–41 cm. **3.** Early cemented siliceous sponge (lithistid) enveloping a bioclast. The lithistid mummy (tuberoid) is formed by early micritic cementation that calcitizes the spicules, thereby preventing disassembly, and leading to a good preservation of the slack spongial structure. Sample 103-639D-5R-2, 94–97 cm. **4.** Detail of tuberoid, with the irregular form inherited from the patchy early micritic cementation.

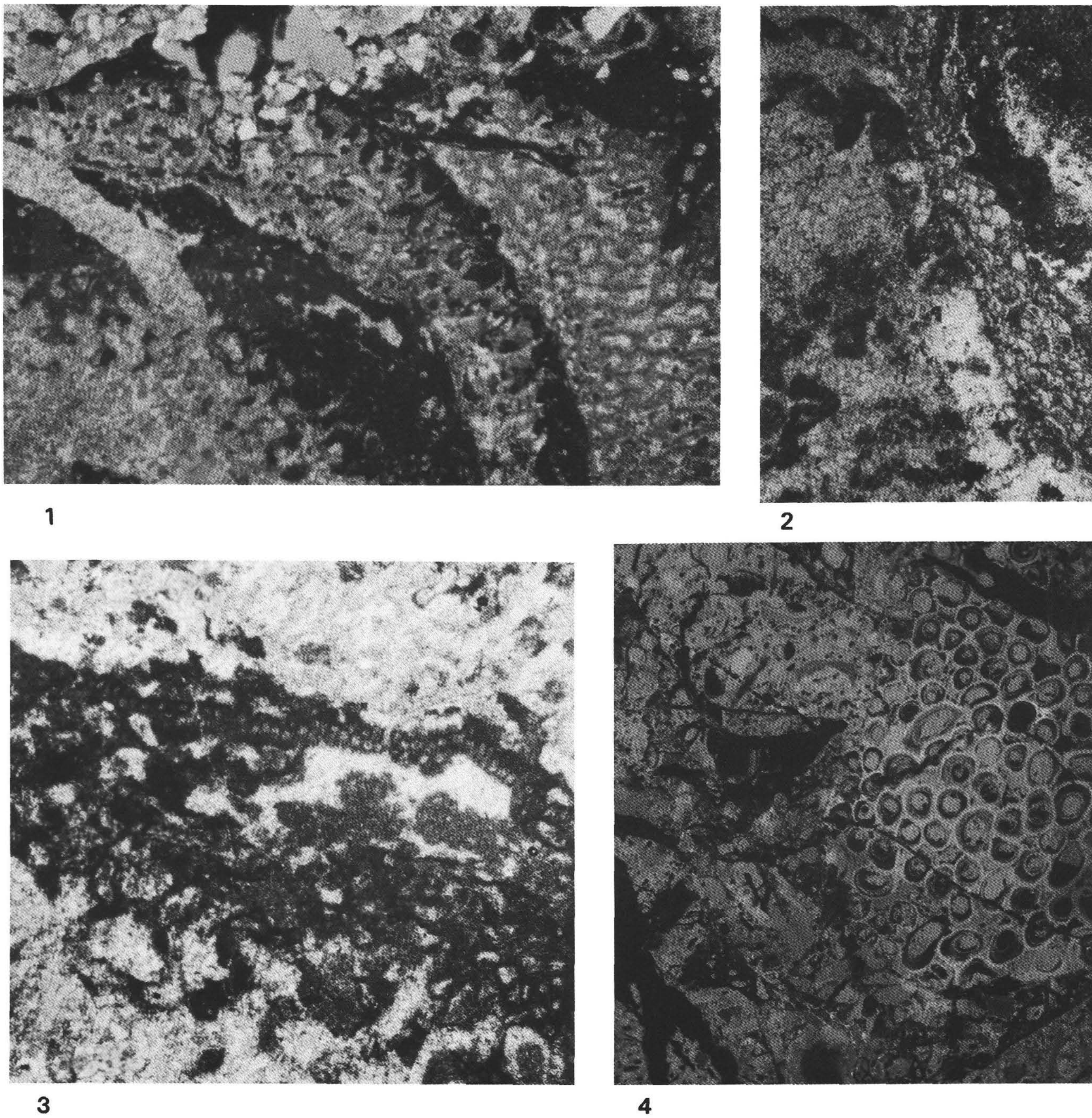

Plate 8. **1.** Fragment of coral (at lower left) coated with polyphased encrustation composed of successive micritic and algal layers and Chaetetid growth. Sample 103-639D-5R-3, 42–44 cm (15X). **2.** Coral fragment encrusted by stromatoporids(?). Sample 103-639D-5R-1, 26–29 cm (25X). **3.** Detail of part of the micritic encrustation in Figure 1, showing a heterogenous micritic and cellular (*Thaumatoporella*-type) coating. Sample 103-639D-5R-3, 42–44 cm (36X). **4.** Repeated sections through an annelid tube. Sample 103-639D-5R-2, 60–62 cm (Negative print from thin section. 7X).

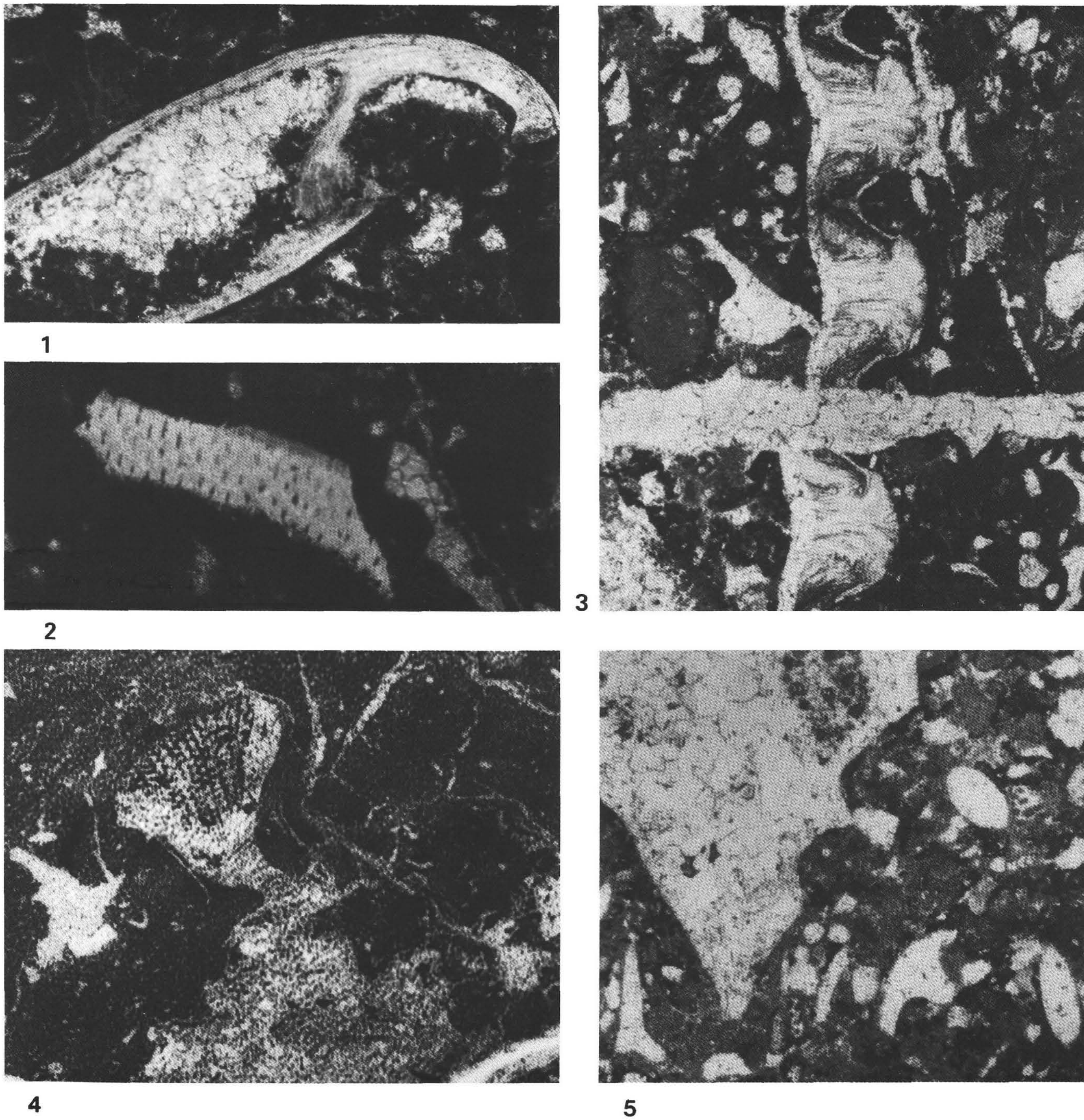

Plate 9. **1 and 2.** Sample 103-639D-5R-2, 60–62 cm (36X). Figure 1 shows partial transverse section of a punctuate brachiopod with the brachial crura of the dorsal shell. Figure 2 is a tangential section of a punctuate brachiopod shell fragment showing well-delineated pores. **3–5.** Sample 103-639D-5R-2, 63–65 cm (3X). Figure 3 shows a pelecypod microstructure of pectinid type in the same matrix as Figures 1 and 2. Figure 4 is of a small coral in life position. Figure 5 shows the micritic matrix, including numerous dispersed calcitized sponge spicules and a few bioclasts (especially gastropods).

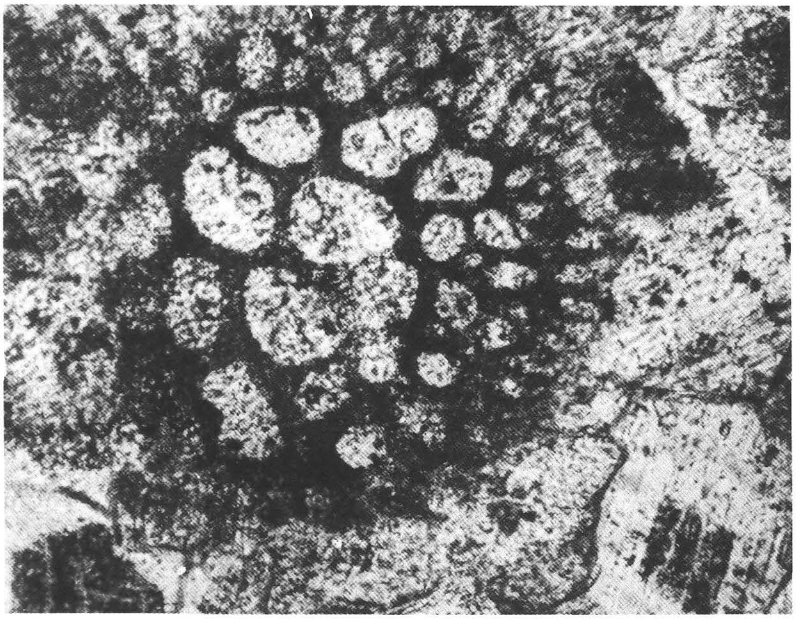

1

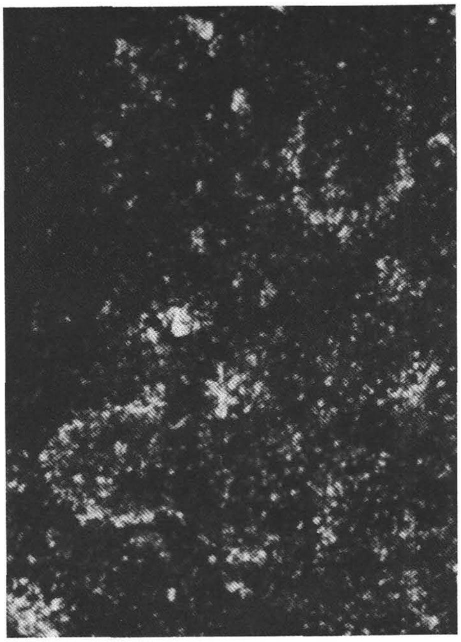

2

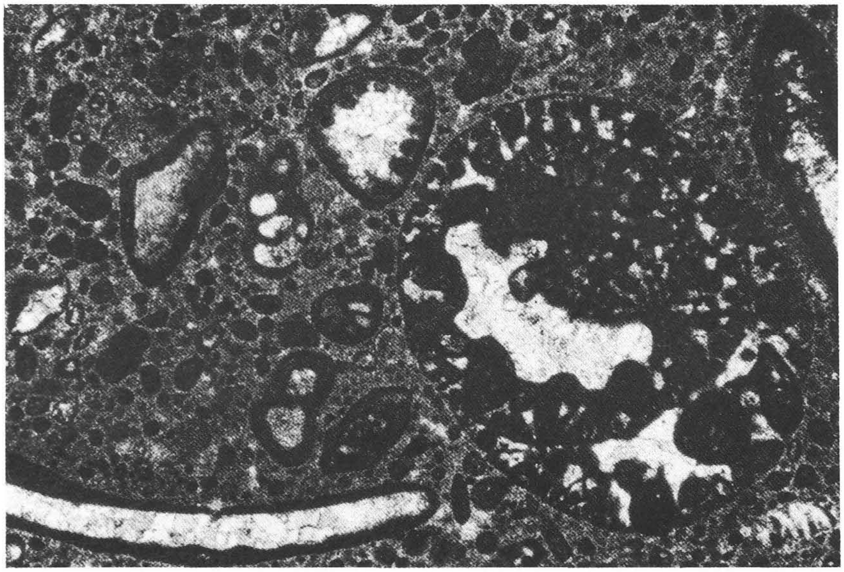

3

4

Plate 10. **1.** Dolomite with a tangential section of *Anchispirocyclina*. Sample 103-639A-10R-2, 52–56 cm (80X). **2.** Heavily recrystallized Calpionellids (?*Crassicollaria*). Sample 103-639D-5R-1, 105–108 cm (32X). **3.** *Pseudocyclammina lituus*, *Trocholina alpina*, and other benthic foraminifers and encrusted pelecypod fragments in a heterometric packstone. Sample 103-639D-13R-1, 117–120 cm (8X). **4.** Axial section of *Nautiloculina oolithica*. Sample 103-639D-13R, CC (20X).

1

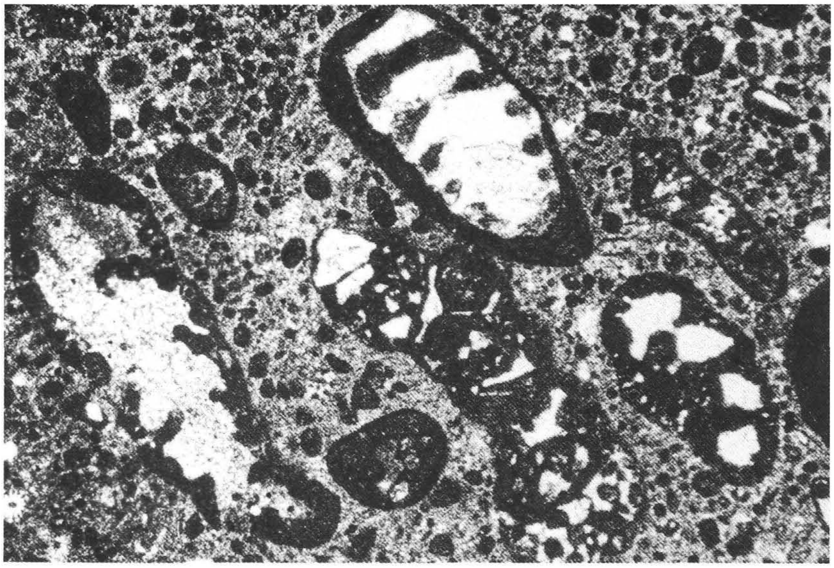

2

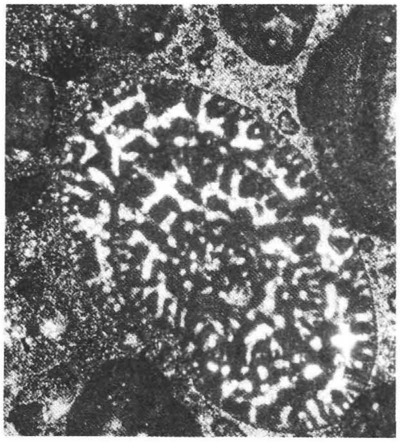

3

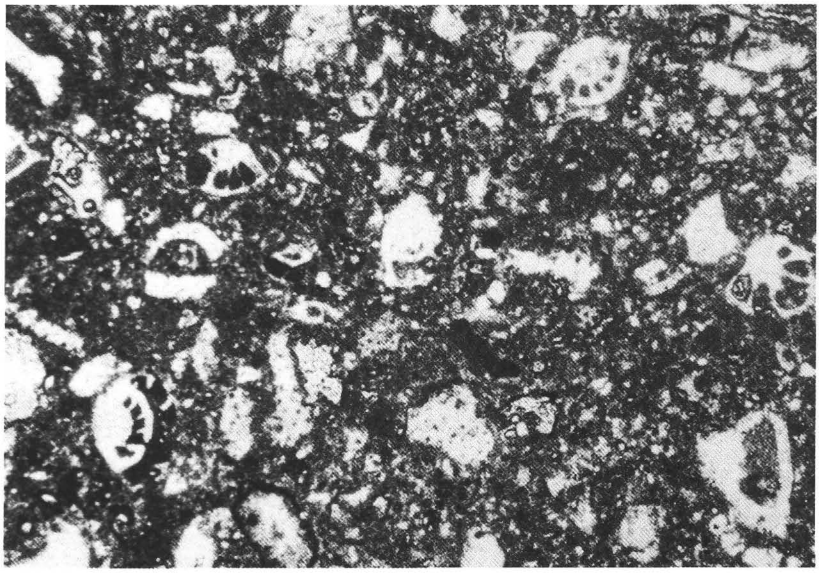

4

Plate 11. (35X unless noted otherwise). **1.** An isolated abraded specimen of *Anchispirocyclina lusitanica* showing the subepidermal structure. Sample 103-639D-7R-1, 142–134 cm (5X). **2.** Clotted microfacies with abundant benthic foraminifers, including *Trocholina elongata*, *Pseudocyclammina lituus*, and indeterminate Pseudocyclamminids. Sample 103-639D-13R-1, 117–120 cm. **3.** Subaxial section of *A. lusitanica*. Sample 103-639D-13R-2, 72–76 cm. **4.** Epistominids and other calcareous biogenic debris. Sample 103-639D-6R-1, 60–66 cm.

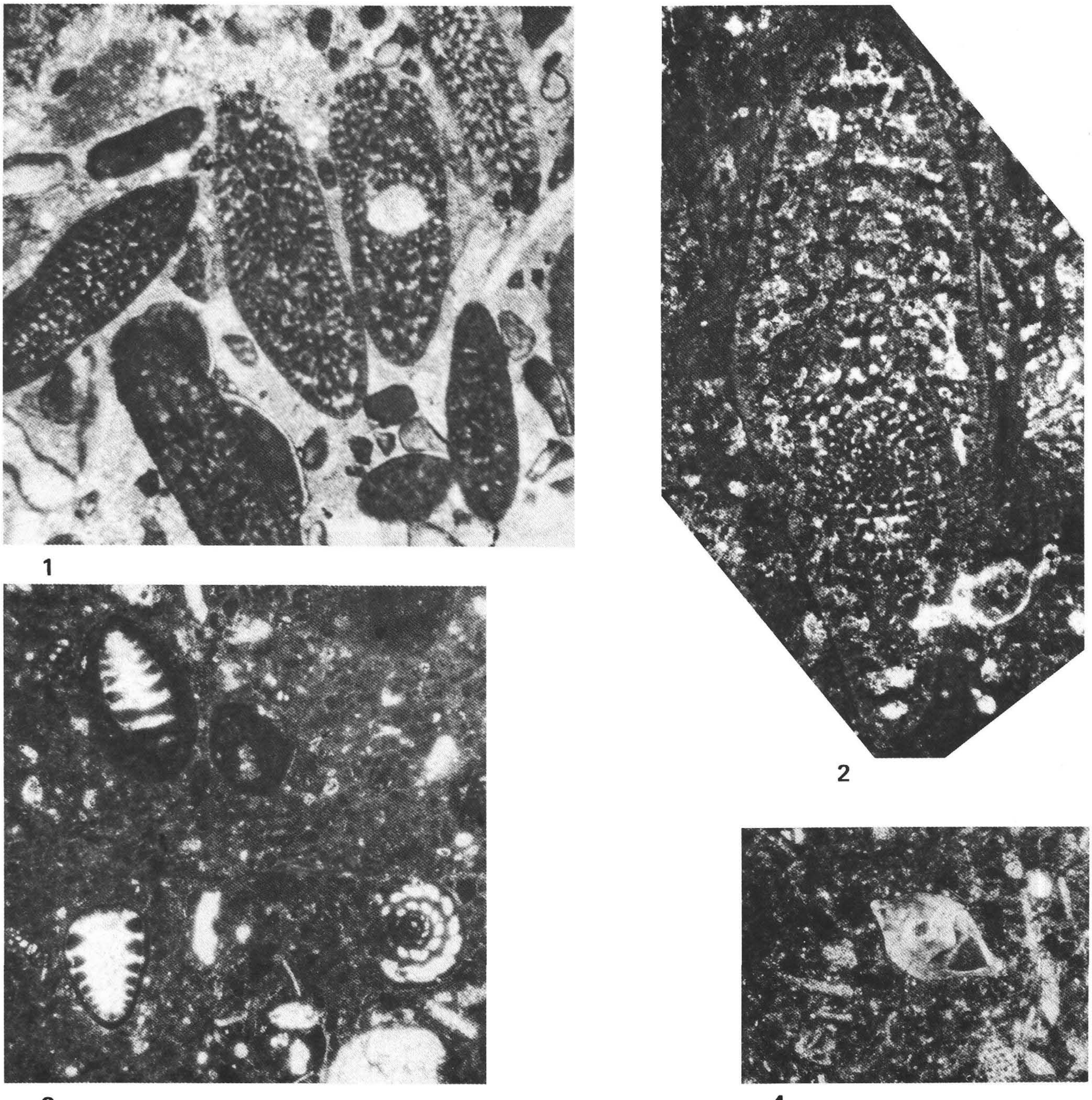

Plate 12. (8X). **1.** *Anchispirocyclina lusitanica*. Note the embryonic chamber (filled with sparite) in the megaspheric specimen on the right side of the figure. Sample 103-639D-7R-1, 71–75 cm. **2.** An almost axial section of *A. lusitanica*. Sample 103-639D-12R-1, 27–31 cm. **3.** *Trocholina elongata* and *Nautiloculina oolithica* (horizontal section) in a micropackstone matrix showing pellets with blurred contours. Sample 103-639D-13R-1, 117–120 cm. **4.** *Lenticulina* sp. (axial section). Sample 103-639D-5R-1, 55–57 cm.

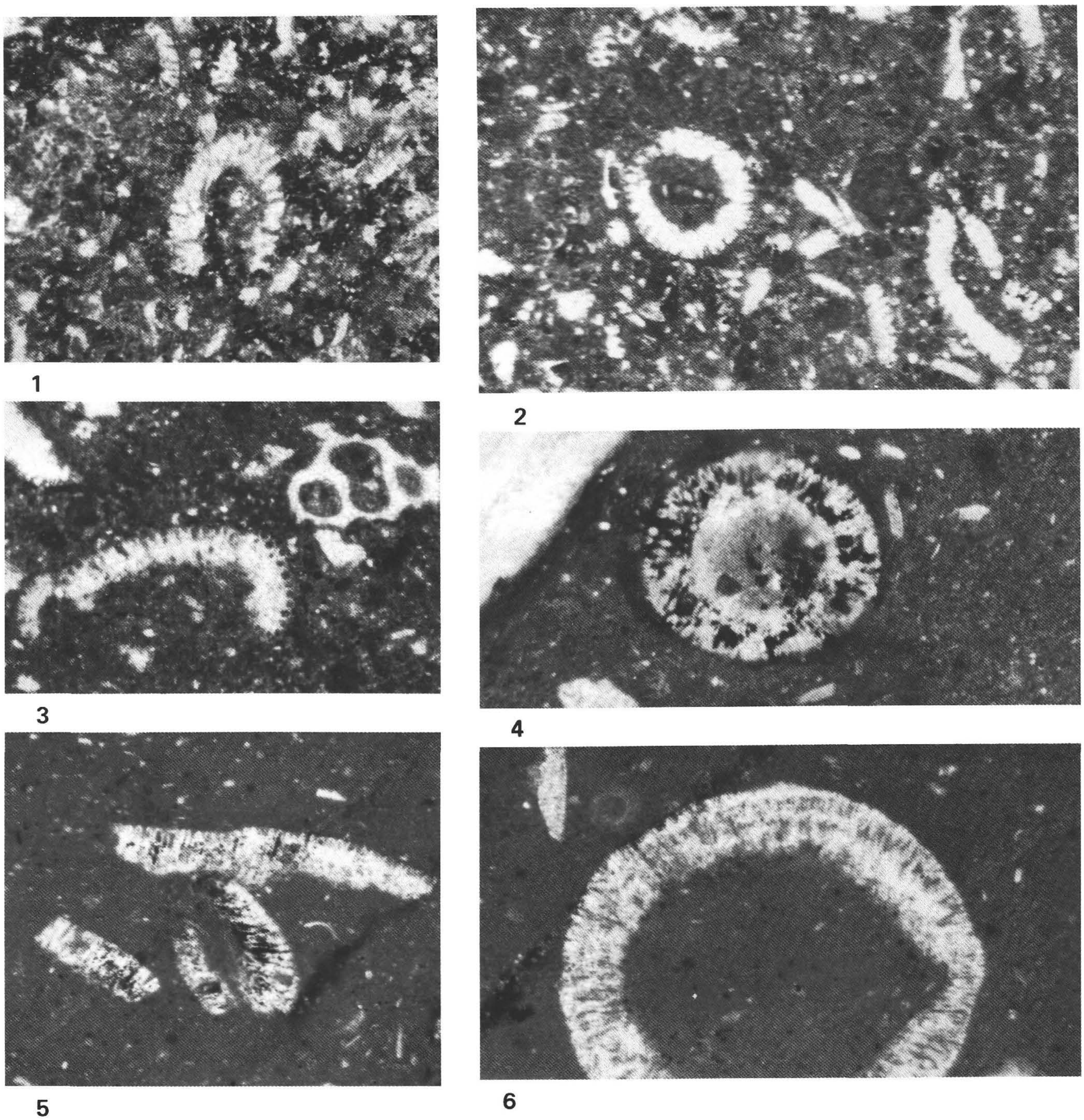

Plate 13. (40X). Transverse and oblique sections of Chlorophycean-Udoteacean algae (*Arabicodium*) in a wackestone texture. Bioclasts are homogenous and were probably not reworked. **1.** Sample 103-639D-6R-1, 60–66 cm. **2 and 3.** Sample 103-639D-6R-1, 90–96 cm. **4.** Sample 103-639D-10R-1, 39–42 cm. **5 and 6.** Sample 103-639D-10R-1, 100–104 cm.

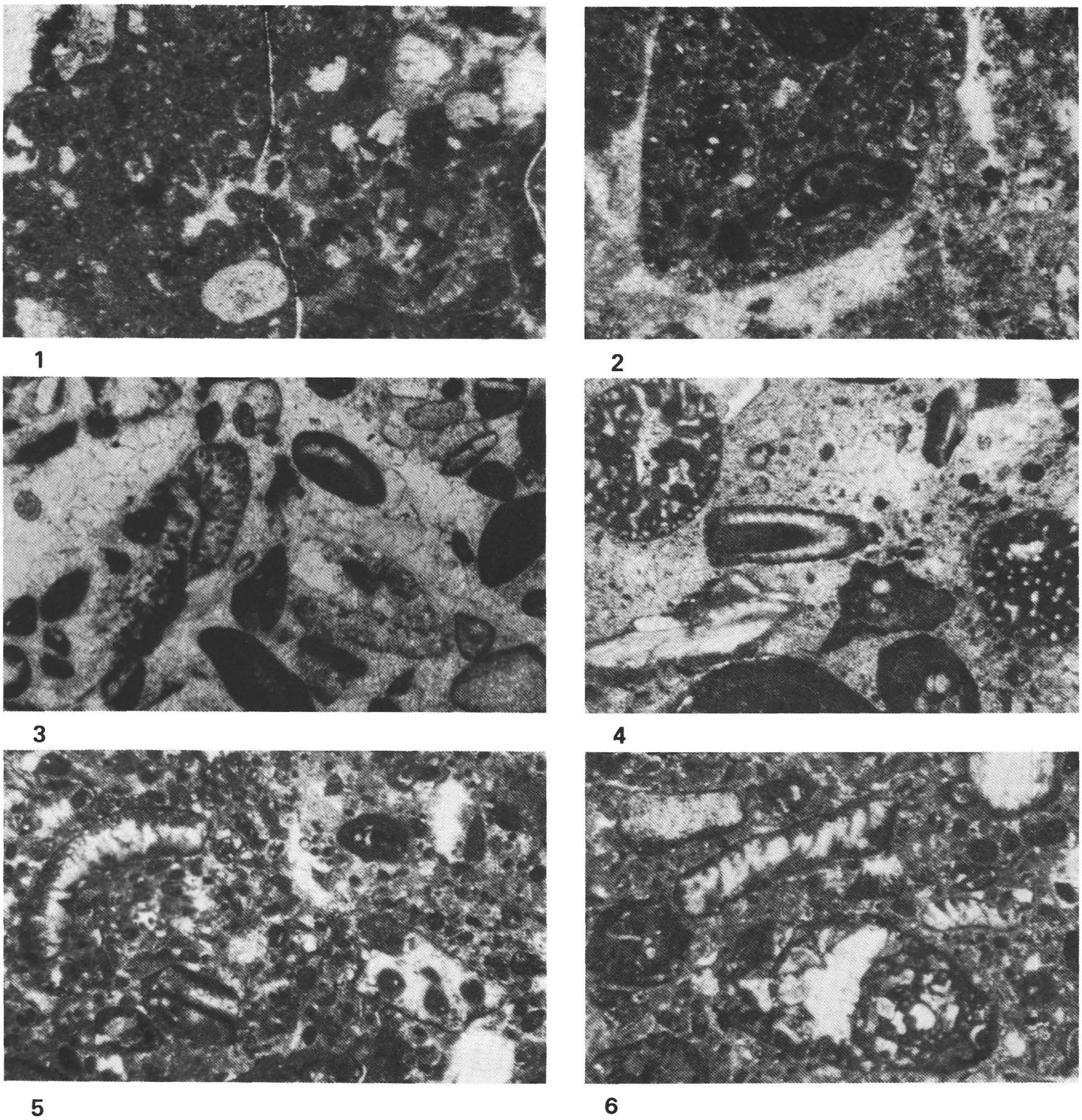

Plate 14. Algal (Dasycladacean and Udoteacean) debris in floatstone (Figs. 1 and 2), grainstone (Figs. 3 and 4), and heterometric packstone (Figs. 5 and 6) textures. The micritic cortex of some algal bioclasts (Figs. 2, 4, and 6) differs from the matrix, which indicates possible reworking. **1.** *Pseudoclypeina*? Sample 103-639D-4R-1, 97–99 cm (40X). **2.** *Clypeina*. Sample 103-639D-6R-3, 53–57 cm (40X). **3.** Sample 103-639D-7R-1, 71–75 cm (40X). **4.** Sample 103-639D-9R-1, 62–64 cm (40X). 5. *Cylindroporella*, Sample 103-639D-12R-2, 85–88 cm (35X). 6. Sample 103-639D-12R-2, 110–114 cm (35X).

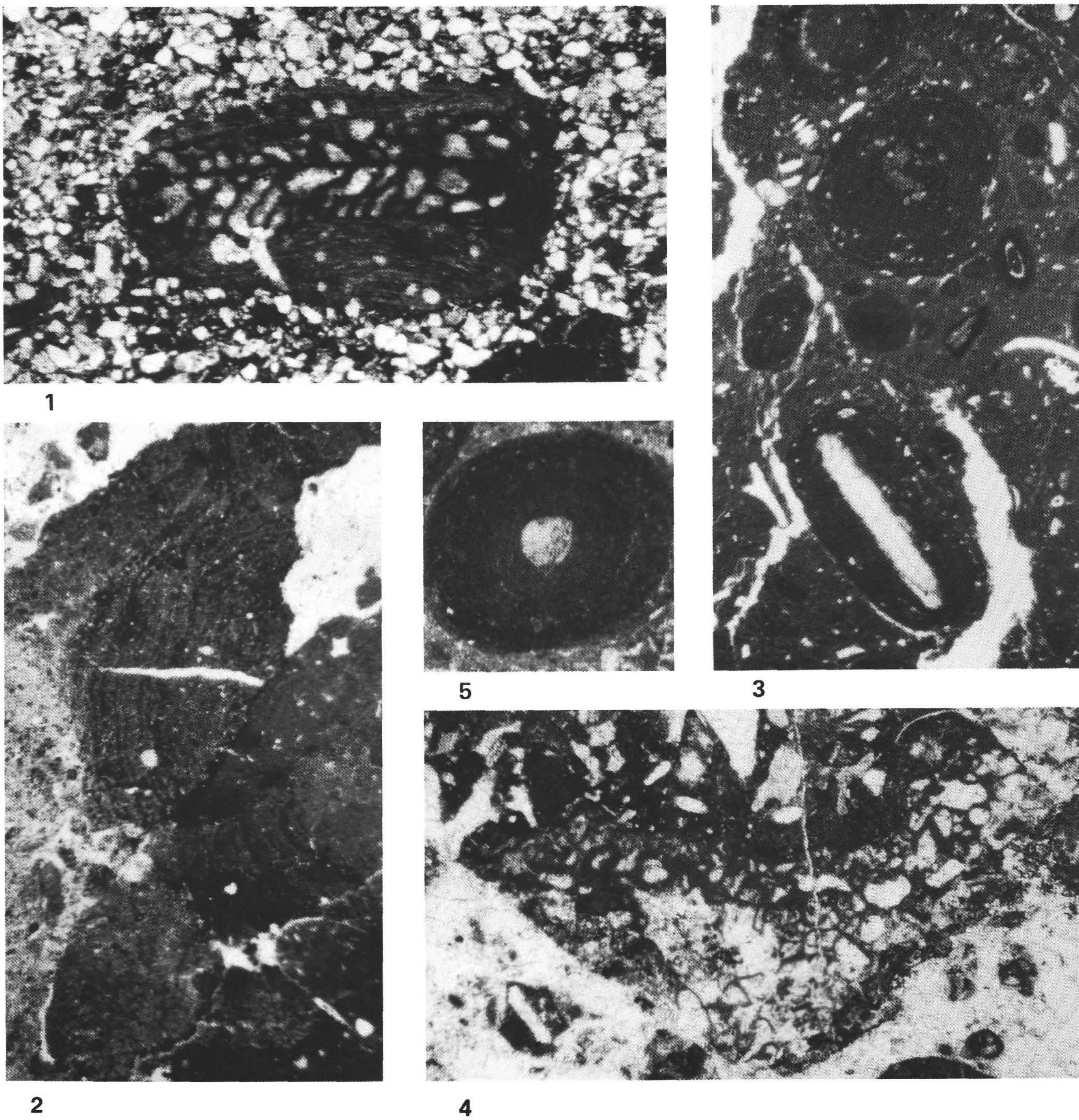

Plate 15. Algal and Cyanobacterian encrustations. **1.** Stromatolitic-like encrustation. Sample 103-639D-4R-1, 42–44 cm (20X). **2.** *Bacinella* or "*Lithocodium*" structure, interpreted as a Cyanobacterian or stromatoporid construction. Sample 103-639D-5R-2, 63–65 cm (30X). **3.** *Bacinella* debris with an algal(?) cortex in a very fine-grained sandstone. Sample not identified (40X). **4.** (Sample 103-639D-13R-1, 128–133 cm, 10X) and 5 (Sample 103-639D-8R-1, 74–79 cm, 40X). Oncoidal structures showing a densely laminated micritic cortex of algal (Cyanophycean or Cyanobacterian) origin.